A Mathematical Description of the Control System for the William Herschel Telescope

R.A. Laing,
Royal Greenwich Observatory,
Madingley Road,
Cambridge CB3 0EZ.

Abstract

The algorithms used to convert between coordinates of an astronomical object given in a standard system and the demand position and velocity output to the telescope servo system are described in detail. Novel features of the WHT control system are emphasised, in particular the methods used to correct for errors in the different encoding systems, the control of derotation optics and the rotator and azimuth limit calculations.

1 Introduction

Precise control is critical to the pointing, tracking and imaging of modern telescopes. The control system developed for the William Herschel Telescope (WHT) has met stringent performance targets and its conceptual framework is adequate for the yet more demanding requirements of the Gemini project. The purpose of the present paper is to describe the algorithms used in the WHT control system, without much reference to details of implementation. The aims are to document the existing code and to provide a starting point for specification of a new implementation using different hardware, language and operating system.

The WHT is a 4.2-metre telescope with an altazimuth mount. It has four focal stations: Prime, Cassegrain and two Nasmyth. The Telescope Control System (TCS) is the software required to point the telescope at an astronomical object, to track and focus it accurately and to make any offsets necessary during the observation. The mechanisms to be controlled are therefore: altitude and azimuth drives, instrument rotation at each of the four focal stations, secondary mirror tilt, dome, shutters, primary mirror cover and focus. Acquisition cameras and autoguiders are not under the control of the TCS, but provide data to it.

The TCS is implemented in FORTRAN (with a minimum of Macro and C) on a Vax 4000-200 minicomputer. It is interfaced to the telescope hardware via Camac and to the autoguiders and acquisition cameras using serial lines. It may be operated either in stand-alone mode or from the system computer, to which it is interfaced using Decnet from an ADAM D-task.

Section 2 summarises the basic geometry for an altazimuth telescope and derives velocities and accelerations, which are needed in order to estimate the necessary update rates for pointing calculations.

The tangent-plane coordinate systems used later are also defined. Section 3 describes the transformation between astronomical coordinates and the mount altazimuth system and section 4 outlines the processing of encoder and transducer readings and the calculation of drive demands. The derivation of the quantities shown on the Information Display is the subject of section 5; this is mostly concerned with software limits. Section 6 outlines calibration and diagnostic procedures and section 7 suggests some directions for future development of the system.

A glossary of the symbols used is given in Appendix A. The sections of the William Herschel Telescope Users' Manual describing the TCS are attached as Appendices B – E. These give a complete specification of the system commands and display output. Their contents are: classified command summary (Appendix B), alphabetical glossary (Appendix C), interactive control using the TCS "handset" (Appendix D) and the Information Display (Appendix E).

The algorithms used for autoguiding are described elsewhere (Laing 1993; hereafter *AG*). Extensive reference is also made to the *Explanatory Supplement to the Astronomical Almanac* (Seidelmann 1992), hereafter *Explanatory Supplement*. The sign conventions for astronomical coordinates are those used in this reference:

1. Azimuth (A) is measured from north through east in the plane of the horizon and elevation (E) or altitude is measured perpendicular to the horizon ("elevation" and "altitude" are used interchangeably, following conventional usage). Zenith distance $z = \pi/2 - E$ is more often used in calculations, since it is a natural polar coordinate. Note that Wallace (1990) measures azimuth from south though east.

2. Hour angle (h) is measured westwards in the plane of the equator from the meridian and declination (δ) is measured perpendicular to the equator, positive to the north.

3. Right ascension (α) is measured from the equinox eastward in the plane of the equator.

4. Longitude is measured from the equinox eastward in the plane of the ecliptic and latitude (ϕ) is measured perpendicular to the ecliptic, positive to the north.

5. Sky position angle (PA), θ, is measured anticlockwise from north.

2 Basic Geometry

2.1 Equatorial to Altazimuth Conversion

In this section, we summarise the conversions between equatorial (h, δ, θ) and altazimuth (A, z, ϕ) coordinates and the velocity and acceleration on the sky in the latter system during sidereal tracking. ψ is the parallactic angle, *i.e.* the angle between the projections on the of the local vertical and the meridian. The conversions are contained in equation 4.5.17 of Murray (1983):

$$\begin{aligned}
\cos z &= \cos\delta\cos h\cos\phi + \sin\delta\sin\phi \\
\sin A\sin z &= -\sin h\cos\delta \\
\cos A\sin z &= \sin\delta\cos\phi - \cos\delta\cos h\sin\phi \\
\sin\psi\sin z &= \cos\phi\sin h \\
\cos\psi\sin z &= \cos\delta\sin\phi - \sin\delta\cos\phi\cos h
\end{aligned}$$

The definition of sky PA is instrument-dependent, and a spectrograph slit or one of the detector axes is generally used as a reference. The mount position angle, ρ, measures the rotation of a direction

fixed in the rotator around the optical axis of the telescope anticlockwise from the vertical direction. In order to maintain a fixed relation between mount and sky position angle for different configurations, the WHT control system has an offset parameter, θ_0, which is an instrument-dependent constant. The relation between sky PA, mount PA and parallactic angle, ψ is then:

$$\rho = (\theta - \theta_0) - \psi$$

for Cassegrain and Prime foci and

$$\rho = (\theta - \theta_0) - \psi \pm E$$

for the Nasmyth foci (+ for the UES and − for the GHRIL focal stations).

2.2 Velocities and accelerations

The first derivatives of azimuth, zenith distance and parallactic angle are required in order to estimate the update rates required for pointing calculations. Primes denote differentiation with respect to hour angle. In order to get derivatives with respect to sidereal time, we need to multiply by μ or μ^2 for first and second derivatives, respectively, where μ is the sidereal tracking rate, 7.272 $\times 10^{-5}$ rad s^{-1}.

2.2.1 Zenith distance

$$-z' \sin z = -\cos\phi \cos\delta \sin h$$

and therefore the elevation velocity is

$$z' = \cos\delta \cos\phi \sin h / \sin z = -\sin A \cos\phi$$

A further differentiation gives

$$(z')^2 \cos z + z'' \sin z = \cos\phi \cos\delta \cos h$$

and the acceleration is

$$z'' = \cos\phi(\cos\delta \cos h - \sin^2 A \cos\phi \cos z)/\sin z$$

2.2.2 Azimuth

$$\sin z \sin A = -\sin h \cos\delta$$

$$\begin{aligned} z' \cos z \sin A + A' \cos A \sin z &= -\cos h \cos\delta \\ &= \sin z \cos A \sin\phi - \cos\phi \cos z \end{aligned}$$

and the azimuth velocity is therefore

$$A' = (\sin\phi \sin z - \cos\phi \cos z \cos A)/\sin z$$

The maximum velocity is 1 deg s^{-1}, so the radius of the "blind spot" at the zenith is 0.21°. A convenient way of writing A' is in terms of the parallactic angle, ψ, using the expression derived in the next subsection:

$$\sin\psi = -\sin A \cos\phi / \cos\delta$$

$$\cos\psi\psi' = -\cos AA'\cos\phi/\cos\delta$$
$$\psi' = -\cos\phi\cos A/\sin z$$
$$\Rightarrow A' = \cos\psi\cos\delta/\sin z$$

Consequently,

$$\begin{aligned} A'' &= \cos\delta\left(\frac{-\sin z\sin\psi\psi' - \cos\psi\cos zz'}{\sin^2 z}\right) \\ &= \frac{\cos\delta\cos\phi}{\sin^2 z}(\cos\psi\cos z\sin A - \sin\psi\cos A) \end{aligned}$$

2.2.3 Parallactic angle

$$\sin z\cos\psi = \sin\phi\cos\delta - \cos\phi\sin\delta\cos h$$

We differentiate this, and substitute for z', using the results of the previous subsection:

$$\begin{aligned} \psi' &= \frac{-\cos\phi}{\sin z\sin\psi}(\sin A\cos z\cos\psi + \sin\delta\sin h) \\ &= -\cos\phi\cos A/\sin z \end{aligned}$$

We then differentiate again and insert the expressions for A' and z' derived earlier:

$$\begin{aligned} \psi'' &= -\frac{\cos\phi}{\sin^2 z}(-\sin z\sin AA' - \cos A\cos zz') \\ &= \frac{\sin A\cos\phi}{\sin^2 z}(\cos\psi\cos\delta - \cos A\cos z\cos\phi) \end{aligned}$$

2.2.4 Recalculation of the velocity demand

The position error can be estimated by expanding the quantity concerned in a Taylor series:

$$x(h+\Delta h/2) = x(h) + x'(h)(\Delta h/2) + x''(h)(1/2)(\Delta h/2)^2 + ...$$

If the velocity demand is $x'(h)$, *i.e.* that appropriate to the middle of the period $h - \Delta h/2 - h + \Delta h/2$, then the error at the end of the period is given to a first approximation by:

$$x(h+\Delta h/2) - [x(h) + x'(h)(\Delta h/2)] \approx x''(h)(\delta h^2/8)$$

We wish to ensure that, within the allowed rate of the telescope ($0.2° < z < 80°$), the rate of recomputation of velocity is not the main factor affecting the timing of the servo loop (an update rate of 20 Hz is justified by the mechanics of the telescope). We use the expressions for the second derivatives of A, z and ψ calculated above. The worst cases occur near the zenith, and are approximate by $\mu^2/\sin z$ in A and z and by $\mu^2 r/\sin^2 z$ for ψ, where r is the field radius. The maximum positional error for an update rate of 20 Hz is then roughly 0.002 arcsec for A and z and 0.004 arcsec for ψ (at a field radius of 30 arcmin). These numbers are negligible compared to other sources of error in the present case.

2.3 Coordinates in the tangent plane

A common requirement is to move the telescope in such a way that an image moves by a given distance on the detector. The appropriate formulae (assuming a constant plate scale) are those for gnomonic projection onto a tangent plane (*e.g.* Murray 1983). A similar application is to offset the telescope by a given angular distance on the sky. Since the $\alpha\delta$ and Az coordinate systems are both polar, a given offset in α or A does not, of course, correspond to the same angular distance everywhere on the sky (*e.g.* it causes no movement on the axis of the coordinate system). The tangent-plane approximation is also suitable for this application and is well-behaved near the pole and zenith. The TCS uses angular units throughout, and the conversion between linear units on the detector and angular units on the sky is implicit in these equations. Three systems are used:

Equatorial Cartesian coordinates ξ and η are defined along the projected $+\alpha$ and $+\delta$ directions at the tangent point (α_0, δ_0):

$$\begin{aligned}
\tan(\alpha - \alpha_0) &= \xi \sec\delta_0/(1 - \eta\tan\delta_0) \\
\alpha - \alpha_0 &\approx \xi \sec\delta_0 \\
\tan\delta &= (\eta + \tan\delta_0)\cos(\alpha - \alpha_0)/(1 - \eta\tan\delta_0) \\
&= (\eta + \tan\delta_0)/[(1 - \eta\tan\delta_0)^2 + \xi^2\sec^2\delta_0]^{1/2} \\
\delta - \delta_0 &\approx \eta
\end{aligned}$$

where the approximations are the usual ones for small displacements at positions well away from the pole.

Altazimuth An equivalent pair of coordinates σ, τ is defined in the altazimuth system, with σ along the $+A$ direction and τ along $+E$ at the tangent point (A_0, E_0) (note that the handedness is opposite to that of the equatorial system).

$$\begin{aligned}
\tan(A - A_0) &= \sigma \sec E_0/(1 - \tau\tan E_0) \\
A - A_0 &\approx \sigma \sec E_0 \\
\tan E &= (\tau + \tan E_0)\cos(A - A_0)/(1 - \tau\tan E_0) \\
&= (\tau + \tan E_0)/[(1 - \tau\tan E_0)^2 + \sigma^2\sec^2 E_0]^{1/2} \\
E - E_0 &\approx \tau
\end{aligned}$$

xy Finally, x and y are defined along axes fixed with respect to a stationary instrument rotator for a virtual telescope (*i.e.* in the absence of geometrical or flexure errors and refraction). These are used to give a convenient system for offsetting the telescope interactively and the x and y axes are therefore aligned approximately with obvious directions such as detector axes or a spectrograph slit. This is, however, an approximation to the focal-plane coordinate system x_A, y_A, which is fixed with respect to the structure and therefore includes effects such as field rotation due to differential refraction and the effects of pointing errors. The xy system is rotated from the altazimuth system by the mount position angle, ρ, for a perfect telescope and from the $\xi\eta$ system by the sky position angle θ, corrected for the instrumental offset θ_0.

The conversions between these coordinate systems are simple rotations:

$$x = -\xi\cos(\theta - \theta_0) + \eta\sin(\theta - \theta_0)$$

$$
\begin{aligned}
y &= +\xi \sin(\theta - \theta_0) + \eta \cos(\theta - \theta_0) \\
x &= +\sigma \cos\rho + \tau \sin\rho \\
y &= -\sigma \sin\rho + \tau \cos\rho \\
\xi &= -\sigma \cos\psi + \tau \sin\psi \\
\eta &= +\sigma \sin\psi + \tau \cos\psi
\end{aligned}
$$

for Cassegrain and Prime foci, modified by an additional rotation of $\pm E$ at Nasmyth (Section 2). Complications introduced by field distortions (*e.g.* the radial error typically introduced by refracting field correctors and focal reducers) are discussed in *AG*. The TCS does not currently make any allowance for them.

3 Pointing Calculations

3.1 General

The philosophy adopted for the pointing calculations in the TCS is that of the "virtual telescope" (Straede & Wallace 1976), whose imperfections such as flexure and refraction are concealed from the user. All of the control is specified in terms of standard astronomical coordinate systems (for targets) or detector coordinates (for images) The majority of this section is concerned with the conversion between input positions and the (necessarily imperfect) measured coordinates of the mount. Mechanism control and the modelling of imperfections in the encoders are treated in the following section. Sections 3.2 – 3.11 describe aspects of the calculations in detail, whilst Section 3.12 summarises the whole sequence.

In what follows, we refer to the input coordinate system (α, δ and θ as specified by the user) and to mount coordinates (the demand values of A, E (or z) and ρ for the drives). The telescope is driven so as to make the encoder readings for these mechanisms (corrected as described in the next section) identical to these demand values.

3.2 Time

The time calculations performed by the TCS closely follow those given in Chapter 2 of the *Explanatory Supplement* and this section concerns specific details. The times used within the TCS are:

UTC Coordinated Universal Time. This is given directly by the Observatory Time Service.

TAI International Atomic Time. This is calculated from UTC, from which it differs from by a variable integer number of seconds (see below).

TDT Terrestrial Dynamical Time. This is the theoretical timescale of apparent geocentric ephemerides of solar-system bodies and is specified to be TAI + 32.184 s.

TDB Barycentric Dynamical Time is the independent variable of the equations of motion with respect to the solar system barycentre. It is determined from TDT using the expressions given by Moyer (1981).

UT1 Universal Time. This is proportional to the angle of rotation of the Earth in space, reckoned around the true position of the rotation axis. The value of UT1 – UTC is normally entered directly at the start of a night's observing, but by default is calculated using the extrapolation formula given in IERS Bulletin A. The coefficients are stored in the initialization file and should be updated regularly (preferably once per week).

LMST Local Mean Sidereal Time (the hour angle of the mean equinox of date).

LAST Local Apparent Sidereal Time (the hour angle of the true equinox of date). This is determined from UT1 using the formulae of Section 2.242 of the *Explanatory Supplement*. The values for the position of the Pole required in the conversion are either entered directly or calculated using an extrapolation formula, as for UT1 − UTC.

Dates may be specified as in Julian or Besselian years, with the conventional prefixes "J" and "B", as appropriate for the FK5 and FK4 coordinate systems (see below). The standard epochs for the two systems are J2000.0 and B1950.0, respectively.

UTC is kept within 0.9 s of Universal Time (UT1) by the insertion of one-second steps (leap seconds). The procedure for inserting a leap second is as follows:

1. The date at which the leap second is to be inserted is stored (as a modified Julian Date) in the initialization file for the control system.
2. The time service is armed to put in a leap second on that date.
3. The control system then compensates for the effects of the leap second until it is next restarted. The initialization file should then have the new value of UTC - TAI included.
4. Care is needed to ensure that the ERPS coefficients used to extrapolate UT1 − UTC include the effects of the leap second.

3.3 Astronomical Coordinate Systems

3.3.1 General

The TCS accepts input in one of three equatorial coordinate systems:

1. Geocentric apparent coordinates of the current date.
2. Mean coordinates in the post-IAU1976 (FK5) system.
3. Mean coordinates in the pre-IAU1976 (FK4) system.

The procedure used to convert between systems is that described in the *Explanatory Supplement* and in Wallace (1990). The currently-available reference system is based on the FK5 star catalogue, the IAU 1976 set of constants, the IAU 1980 theory of nutation and the set of procedures outlined below. It is in good agreement with the reference frame defined by VLBI observations (although it is expected that further radio observations and data from the Hipparcos satellite will refine the system still further). A considerable number of positions are still given in the older (FK4) system, and routines are provided in the TCS to perform the conversion. The sequence of conversions is FK4 ⇒ FK5 ⇒ apparent. The procedures are unnecessarily rigorous for the application, but do not take significant CPU time: performing calculations to full accuracy makes comparison with standard test cases much more straightforward.

3.3.2 FK4 to FK5 conversion

This procedure is performed once, at the start of a new observation, and produces an FK5 J2000.0 position for the current epoch. An intermediate stage is to calculate the FK4, B1950.0 position:

1. Correct for space motion to the epoch of observation.
2. Remove E-terms of aberration.

3. Precess to B1950.0 using FK4 constants.

4. Add E-terms.

The B1950.0 position is available for display purposes (see below). The position is then transformed to J2000.0:

1. Remove E-terms.

2. Apply space motions to 1984 January 1.0.

3. Precess from B1950.0 to 1984 January 1.0 using the FK4 precession constants.

4. Apply the equinox correction FK4 to FK5 to right ascension and its proper-motion component.

5. Convert the units of proper motion (tropical to Julian centuries).

6. Precess from 1984 January 1.0 to J2000.0

7. Apply space motions to J2000.0

If no proper motions are specified for the FK4 system, then they are assumed to be zero *in the FK5 system.* The distinction is necessary because the FK4 frame rotates slightly with respect to FK5 and it makes more sense to assume that extragalactic objects have no space motions in our best approximation to an inertial frame.

3.3.3 FK5 to geocentric apparent conversion

The first stage is to correct for space motions and to derive a J2000.0 position for the epoch of observation. This is done once, on change of target:

1. Correct for space motions to the epoch of observation.

2. Precess to J2000.0.

3. Correct for parallax.

Conversion to geocentric apparent coordinates is performed continuously during tracking. The conversion matrices are updated once every 5 minutes, but are applied at 20 Hz. The steps are:

1. Correct for gravitational light deflection (negigible in practice).

2. Apply annual aberration.

3. Correct for precession and nutation.

3.4 Offsets

A number of methods are provided to allow offsetting. These are used to move the telescope so that the image of a *different* object appears at the *same* place on the detector and therefore cause the displayed right ascension and declination to change. The opposite approach (moving the image of the *same* object to a *different* place on the detector is described in section 3.7.

3.4.1 RA-Dec offsets

A group of TCS commands deals with differential offsets specified in right ascension and declination. These are applied in the input coordinate system. The first, and simplest, option allows the offset to be given directly as $\Delta\alpha$, $\Delta\delta$, in which case these are merely added to the target position (`OFFSET TIME`). Alternatively, offsets $\Delta\xi$, $\Delta\eta$ in the tangent plane (along the α and δ directions at the target position) may be given, in which case these are converted to $\Delta\alpha$, $\Delta\delta$ using the tangent-plane formulae in Section 2.3 and again added to the target position (`OFFSET ARC`). Tangent-plane offsets may be typed in, stored, listed and applied later (see `ENTER POSITION`, `SHOW POSITION` and `POSITION`); they may also be defined interactively (see below).

3.4.2 The handset

The TCS "handset" (see Appendix D) allows offsets to be introduced interactively using cursor keys. Four modes are associated with offsets: three to implement them in different coordinate systems and the fourth to set them up interactively for storage and later use. Offsets may be applied in $\xi\eta$, xy or $\sigma\tau$ systems as defined in Section 2.3. These are all tangent-plane offsets, so that a given increment causes the image to move by a given amount on the sky at any position. They are applied by rotating to the $\xi\eta$ system, converting to $\Delta\alpha$, $\Delta\delta$ using the formula given in Section 2.3 and incrementing the target position. The accumulated offsets are displayed in the coordinate system of the mode selected. The systems used by the handset are all defined with respect to the input coordinate system, in order to permit easy conversion (a frequent use of the system is to move the telescope in xy coordinates and then to switch to $\xi\eta$ in order to read off the accumulated offset on the sky). A fourth handset mode is used to set up offset positions for later use. An image is placed at some reference point and is then moved to the offset position with the handset. The motion is in the xy system, for convenience, but the offset is stored in $\xi\eta$, so as to be independent of sky position angle.

3.4.3 The blind-offset procedure

A frequent application of the TCS is to acquire faint targets onto an instrument entrance aperture (usually the slit of a spectrograph). The standard procedure is to locate a reference star whose position relative to the target is known very accurately, centre it on the instrument and then offset to the faint target. Although the RA-Dec offsets described above can be used for this purpose, a somewhat different method is neater and more flexible. The reference star is first centred on the instrument, and the accumulated handset correction is converted to tangent-plane coordinates in the mount system and applied as a temporary addition to the collimation errors in elevation and azimuth (Section 3.6.1). This is a local modification to the pointing model which is expected to be valid close to the reference star, and is used for subsequent observations of faint targets. The advantages of this procedure (the `BLIND_OFFSET` command described in Appendix C.10.) are that the target position need not be in the same coordinate system as that of the reference star and that the displayed telescope position is as accurate as possible, rather than including residual pointing corrections.

3.5 Refraction

3.5.1 Refraction formulae

Refraction is treated separately from the other pointing corrections because it is known *a priori*. The algorithm used is derived from the expressions in Murray (1983) for refractive index n and the formulae given by Saastamoinen (1972a, b). Murray's equation 7.4.10 is used to calculate the refractive index as a function of the partial pressures of dry and wet air (in turn derived from the total pressure and

relative humidity), temperature and wavelength. Murray's equation 7.6.8 gives the refraction as:

$$\begin{aligned} z_a - z &= R(z_a) = R_A \tan z_a + R_B \tan^3 z_a \\ R_A &= n - 1 - I \\ R_B &= -[I - (n-1)^2/2] \end{aligned}$$

where the apparent and true zenith distances are z_a and z, respectively and I is the integral of $\ln(n)/s$ over path length s. Saastamoinen (1972a, b) gives simple approximations to I which can be absorbed into the coefficients R_B, R_C, R_D and R_E to give a formula:

$$z_a - z = R(z_a) = R_A \tan z_a + R_B \tan^3 z_a + R_C \tan^5 z_a + R_D \tan^7 z_a + R_E \tan^9 z_a$$

This algorithm gives results within 0.1 arcsec of the numerical integration presented in the *Explanatory Supplement* for z <80°. The refraction formula as quoted is not in a suitable form for pointing calculations, since the refraction is required in terms of the true zenith distance z. We thefore expand $R(z_a)$ in a Taylor series to first order:

$$z \approx z_a + R(z) + (z_a - z)R'(z)$$

and derive the approximate formula

$$\begin{aligned} z - z_a &\approx R(z)/[1 + R'(z)] \\ &= \frac{R_A \tan z + R_B \tan^3 z + R_C \tan^5 z + R_D \tan^7 z + R_E \tan^9 z}{1 + \sec^2 z(R_A + 3R_B \tan^2 z + 5R_C \tan^4 z + 7R_D \tan^6 z + 9R_E \tan^8 z)} \end{aligned}$$

Further elaboration is not justifiable, since accurate measurements of refraction at the CAMC (Morrison, *private communication*) show unpredictable night-to-night variations of up to 0.4tan z arcsec.

3.5.2 Differential refraction

In addition to the effects of refraction on the target position, the field is rotated and distorted. The latter effect can only be corrected using additional optics (as is done at Prime focus), but the former may be taken out using the instrument rotator. This is done automatically as part of the pointing calculation described in Section 3.12, but the analytical treatments in the literature (Hinks 1898, Wallace & Tritton 1979) use obscure notation and a paraphrase is given here using the teminology of the present paper.

Consider a tangent-plane projection (σ, τ) as defined earlier. Then:

$$\sigma = \sin(A - A_0) \csc z_0 / [\cot z \cot z_0 + \cos(A - A_0)]$$

$$\tau = [\cot z - \cot z_0 \cos(A - A_0)] / [\cot z \cot z_0 + \cos(A - A_0)]$$

The effect of refraction is to decrease the value of z, leaving A unchanged. The changes in σ and τ may be calculated from:

$$\begin{aligned} \Delta\sigma &\approx (\partial\sigma/\partial z)\Delta z \\ &= [\csc z_0 \cot z_0 \csc^2 z \sin(A - A_0)] / [\cot z \cot z_0 + \cos(A - A_0)] \\ &= \cos z_0 \csc z \sigma (1 + \sigma^2 + \tau^2)^{1/2} \\ \Delta\tau &\approx (\partial\tau/\partial z)\Delta z \\ &= -[\csc^2 z \csc^2 z_0 \cos(A - A_0)] / [\cot z \cot z_0 + \cos(A - A_0)] \\ &= -(1 + \sigma^2 + \tau^2) \cot z \tan z_0 + \tau(1 + \sigma^2 + \tau^2)^{1/2} \sec z_0 \cos z \end{aligned}$$

In the linear approximation, which is entirely adequate here, we take $\Delta z \approx -R_A \tan z$ and neglect any terms that are second order in σ and τ. Then:

$$\Delta\sigma \approx -R_A\sigma$$

$$\Delta\tau \approx +R_A(\tan z_0 - \tau \sec^2 z_0)$$

We now rotate the coordinate system by the parallactic angle ψ. This leads to the relations given by Hinks (1898):

$$\Delta\sigma \approx R_A[X - (1+X^2)\sigma - XY\tau]$$

$$\Delta\tau \approx R_A[Y - XY\sigma - (1+Y^2)\tau]$$

where X and Y are the quantities defined by Hinks (but in terms of h and δ, so his formulae are messy):

$$X = \sin\psi \tan z_0$$

$$Y = \cos\psi \tan z_0$$

The first terms in the expressions for $\Delta\sigma$ and $\Delta\tau$ are just the shifts of the tangent point due to refraction, which is eliminated by moving the telescope, as discussed earlier, and the introduction of ψ makes it obvious that X and Y are components of a vertical displacement resolved along h and δ, respectively. A rotation of the field results from the fact that the projected north-south line is no longer at position angle 0. The pole is at $(0, \cot\delta_0)$ in the tangent plane, but the origin is displaced to (X, Y) by refraction, so the necessary rotator offset $\Delta\theta$ satisfies:

$$\Delta\theta \approx R_A/(\cot\delta_0 - Y) \approx R_A \sin\psi \tan z_0 \tan\delta_0$$

except very close to the pole (Hinks 1898). The implications of differential refraction for off-axis autoguiding are discussed in *AG*.

3.6 The WHT pointing model

A pointing model is a set of analytical functions and look-up tables used to correct for departures from an ideal altazimuth telescope. The pointing model for the WHT uses up to 21 functions, divided into 3 groups: a geometrical model of the telescope, elevation flexure and harmonics of azimuth. Look-up tables in altitude and azimuth are implemented, but are not currently used. The residuals from a fit to a pointing test (see later) typically have an r.m.s. between 0.8 and 1.5 arcsec, depending on seeing conditions, focal station and measurement technique. An example is shown in Figure 1 and the model terms are listed in Table 1 with their names in the notation of the TPOINT analysis package (Wallace 1989), their functional forms, and typical values for the Cassegrain focus (the sign convention appears strange because the TPOINT software uses a different definition of azimuth). Note that some of the terms are now not significantly different from 0, but are retained because they have been needed in the past.

3.6.1 Geometrical and index Errors

This group has 6 terms, all with some geometrical interpretation. The angles between the instrument rotator axis (which defines the fundamental pointing direction) and the normal to the azimuth and elevation axes are known as collimation errors and the residual zero-point corrections are referred to as index errors. The index and collimation errors in elevation are not separable, and are combined in one coefficient. For this reason, and for convenience in updating the model at the start of an observing session, index errors in both coordinates are included in the pointing corrections, despite the fact that

Table 1: The Pointing Model for the WHT.

Term (TPOINT)	Description	ΔA	Δz	Value (arcsec)
IA	Azimuth index	-1	0	0.5
IE	Elevation index	0	-1	6.7
CA	Azimuth collimation	$-\csc z$	0	73.9
NPAE	Non-perpendicularity	$-\cot z$	0	-12.2
AX	NS axis tilt	$-\sin A \cot z$	$\cos A$	34.1
AY	EW axis tilt	$\cos A \cot z$	$-\sin A$	17.2
TF	Hooke's Law flexure	0	$-\sin z$	-18.0
TX		0	$-\tan z$	0.0
HZSZ4		0	$\sin 4z$	0.0
HSCA1		$\cos A$		-1.5
HSSA1		$-\sin A$		-3.3
HZCA1			$-\cos A$	3.0
HZSA1			$\sin A$	-1.6
HSCA2		$-\cos 2A$		1.5
HSSA2		$\sin 2A$		0.3
HZCA2			$\cos 2A$	-0.8
HZSA2			$-\sin 2A$	0.3
HSCA3		$\cos 3A$		0.0
HSSA3		$-\sin 3A$		2.7
HZCA3			$-\cos 3A$	-2.1
HZSA3			$\sin 3A$	0.9

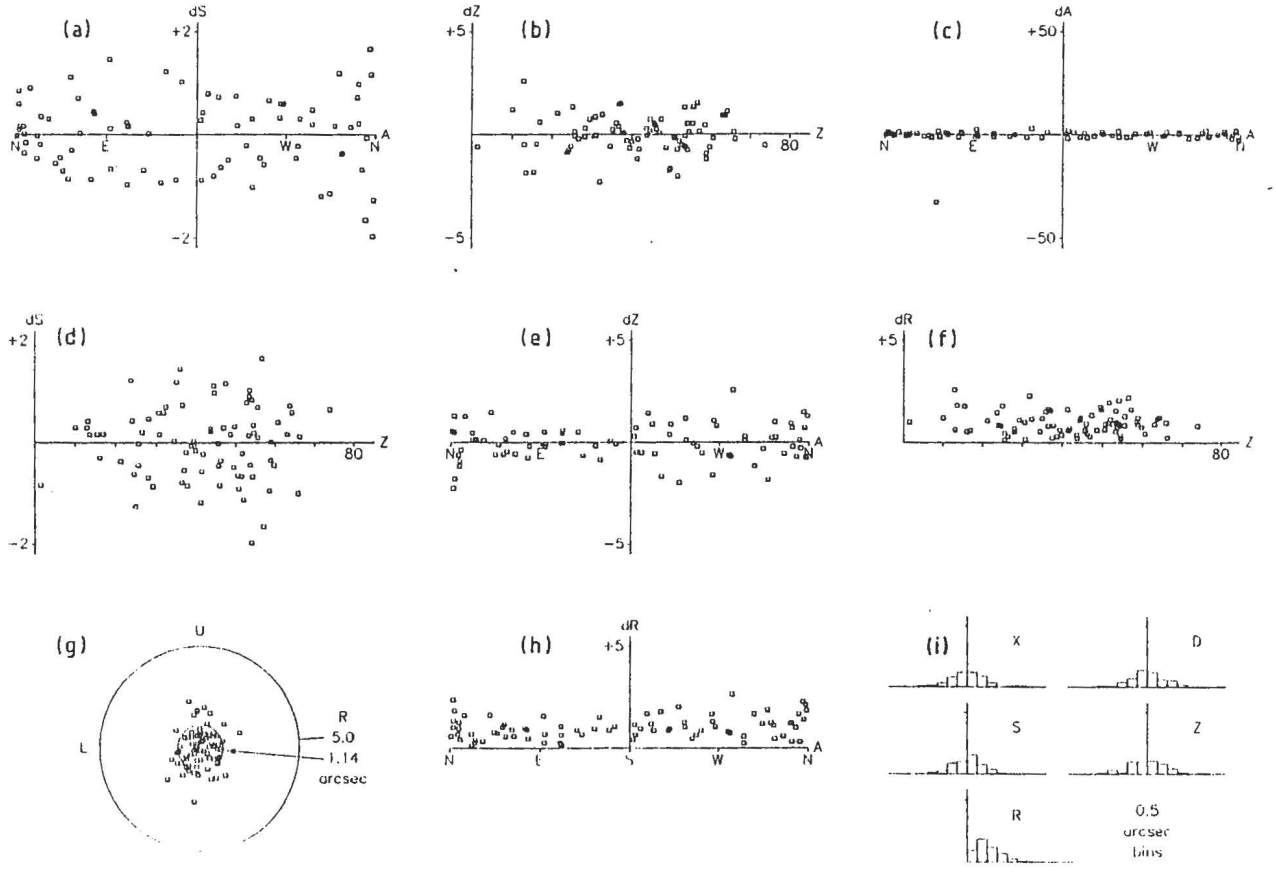

Figure 1: Residuals from a pointing test at the Cassegrain focus. (a) – (f), (h): residuals in $S = A \sin z$, z, A and R (total error) plotted against A and z. Units are degrees on the x axes and arcsec on the y axes. (g) Scatter plot of residuals (U = up; L = left). (i) Histogram of errors in $X = h \cos \delta$, $D = \delta$, S, z and R.

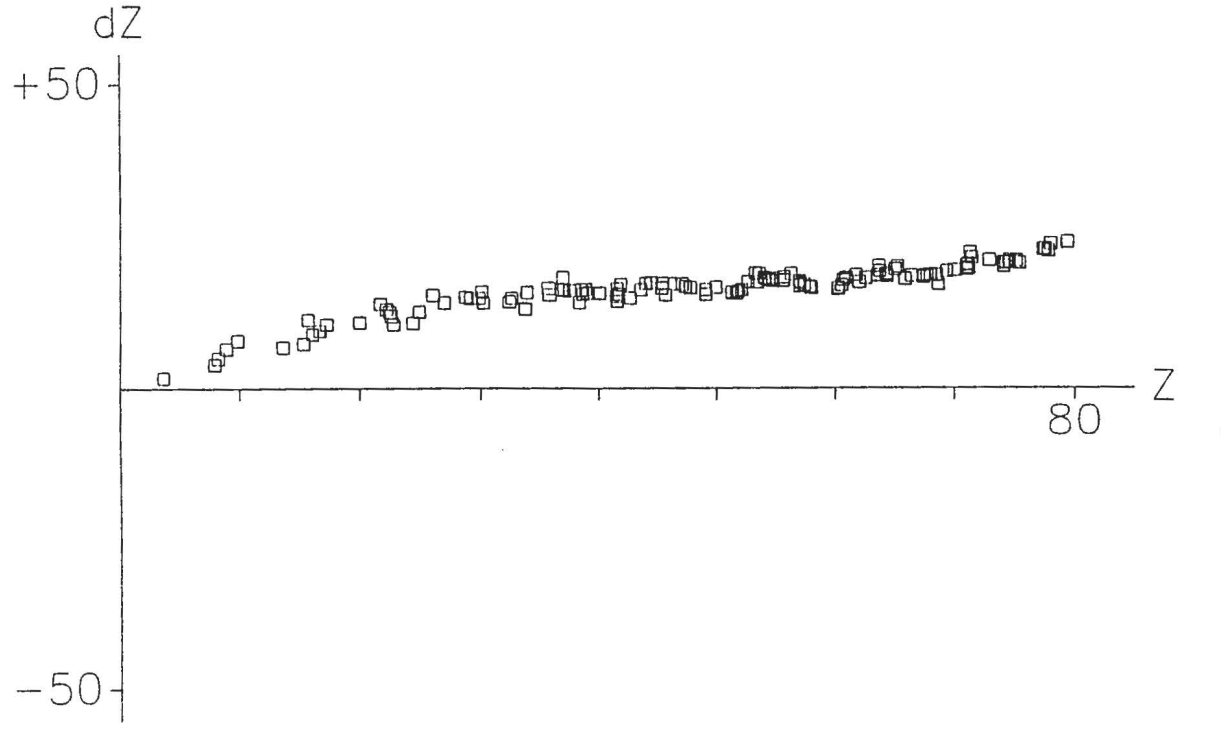

Figure 2: The elevation component of the pointing model for the WHT Cassegrain focus, derived by fitting a model to the data, setting the $\sin z$, $\tan z$ and $\sin 4z$ terms in Δz to 0 and plotting the residuals against zenith distance.

they are logically part of the encoder model (see below). They are kept close to zero by changing the encoder model coefficients. The three simplest terms (elevation and azimuth index errors and left-right collimation) may be updated using the CALIBRATE procedure (see below). The remaining geometrical terms are the non-perpendicularity of azimuth and elevation axes and the tilts of the azimuth axis in the north-south and east-west directions.

It is worth noting that a clock error is equivalent to a tilt of the azimuth axis in the east-west direction, together with an azimuth index error. A 1 s clock error is equivalent to a change in axis tilt by $15\cos\phi$ arcsec and an azimuth offset of $-15\sin\phi$ arcsec. If an error is made in the time (*e.g.* because UT1−UTC is not updated frequently enough, or as a result of time service drift) when the telescope pointing is determined, then it may become absorbed in these coefficients, causing confusion later.

3.6.2 Elevation Flexure

The pointing model includes a number of terms which model the tilt and flexure of the structure. Three of these describe the effects of gravitational deflection on the telescope tube and main mirrors. The biggest effect is due to relative translation of the top and bottom ends. The pointing error is given to a surprisingly good approximation by the $\Delta z \propto \sin z$ (Hooke's Law) relation for a simple beam. The form of the deflection is plotted in Figure 2; it is modelled by an expression of the form $\Delta z = \zeta_1 \sin z + \zeta_2 \tan z + \zeta_3 \sin 4z$.

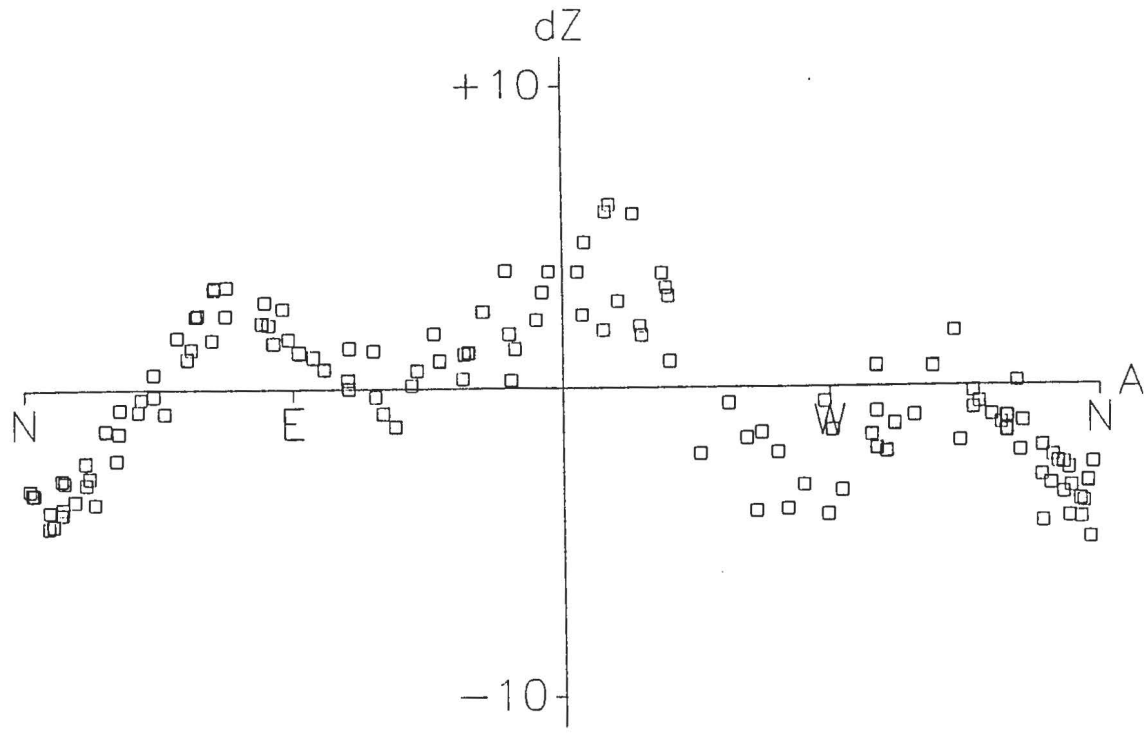

Figure 3: The elevation harmonic component of the pointing model for the WHT Cassegrain focus, derived by fitting a model to the data, setting the harmonic terms to 0 and plotting the residuals in zenith distance against Azimuth.

3.6.3 Azimuth Harmonics

The remaining terms in the pointing model are harmonics of azimuth of the form:

$$\Delta z \propto \sin nA$$

$$\Delta z \propto \cos nA$$

$$\Delta A \sin z \propto \sin nA$$

$$\Delta A \sin z \propto \cos nA$$

where n = 1, 2 or 3 ($\Delta A \sin z$ is the left-right error on the sky). These represent tilts of the entire telescope, due primarily to deviations of the azimuth track from a plane. Their effects are illustrated in Figures 3 and 4.

3.7 The focal-plane coordinate system

It is often necessary to offset the telescope in such a way that an image moves by a given vector in the focal plane, regardless of rotator position angle. The conventional usage for such an operation ("beamswitching" or "aperture offsetting") comes from two-channel photometry. The TCS defines a Cartesian coordinate system (x_A, y_A) in the focal plane for this purpose. If the position angle of the rotator in the mount coordinate system is ρ_M, then the y_A axis is aligned with the vertical direction for $\rho_M = 0$. The origin of the system is fixed by the intersection of the instrument rotator axis of the

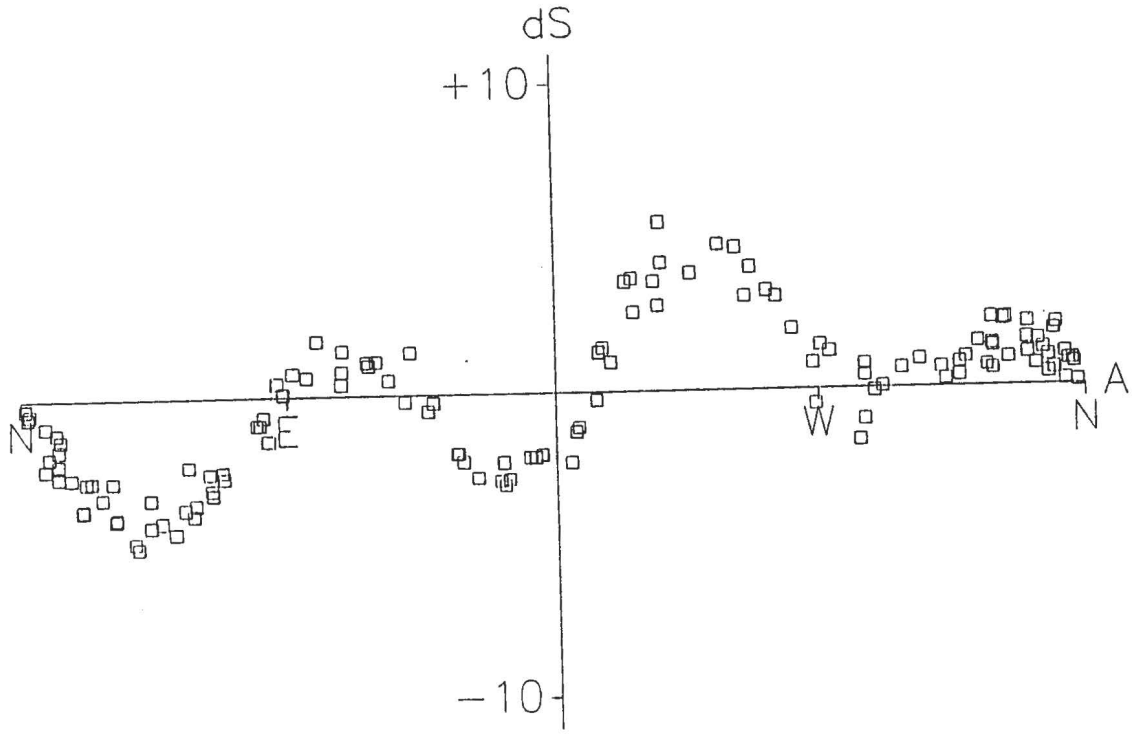

Figure 4: The azimuth harmonic component of the pointing model for the WHT Cassegrain focus, derived by fitting a model to the data, setting the harmonic terms to 0 and plotting the residuals in $\Delta S = \Delta A \sin z$ against azimuth. The mean of the four tape encoder heads was used to measure azimuth for this test.

focal station in use with the focal plane. Positions in this system are referred to as "apertures". If a given (x_A, y_A) offset is introduced, an image coincident with the rotator centre will be moved to a position fixed in the focal plane, independent of sky position angle, θ. Consequently, any movement of the rotator causes the telescope to be offset in such a way that the field appears to rotate about (x_A, y_A). Apertures are numbered from 0 – 10, aperture 0 (the "reference position") being a special case. Aperture 0 is the default on change of source and can be set to some useful position on the instrument, such as the centre of a spectrograph slit or polarimetric dekker. It is particularly important if the instrument is significantly displaced from the axis of rotation. The remaining aperture positions are selectable by the user, as described in Appendix C under the `ENTER`, `STORE`, `APERTURE` and `BEAMSWITCH` commands.

It is possible to define an aperture interactively using a mode of the handset (see Appendix D). An image is centred on the reference position using one of the xy, $\alpha\delta$ or $\sigma\tau$ modes. The handset is then switched to the $x_A y_A$ system and the image is moved to the desired position in the focal plane, which is then kept for latter use. The $x_A y_A$ mode may be used whilst autoguiding, since the position of the guide star on the autoguider CCD is then automatically compensated for motion in the focal plane.

A rotational offset ρ_A may be introduced in an analogous way. This is conceptually a change in the conversion between virtual sky PA and actual mount PA. In the acquisition of a field onto a multislit mask or long slit, for instance, it is necessary to correct for rotational errors (*e.g.* incorrect positioning of the mask in the instrument) as well as translational ones. In addition, some instruments (*e.g.* the Utrecht Echelle Spectrograph) have a rotating slit unit which changes the relation between mount and sky PA. The `TWEAK` command (Appendix C.73) implements an $x_A y_A \rho_A$ offset which also works whilst autoguiding. The xy coordinates for this command may be in a different system from $x_A y_A$, and scale, rotation and handedness conversions are done using instrument-dependent parameters. Thus, for example, the TCS will accept the displacement and rotation output by the LEXT software used for aligning multislit fields.

3.7.1 Rotation and focus

The handset allows the sky PA and focus values to be adjusted interactively.

3.8 Tilt and translation of optical surfaces

Tilts and relative translations of the primary, secondary and tertiary mirrors cause significant pointing errors. The reproducible parts of these errors are taken out by the pointing model, but significant residuals remain. The secondary mirror tilts by small amounts within its cell as the telescope elevation changes (Figures 5 and 6). Since the tilt shows some hysteresis, it is measured using three displacement transducers and corrected as a collimation error rather than being included in the pointing model. A similar technique may be applied in the future to compensate for small tilt errors of the primary mirror measured using the support load cells. Relative translation of the primary and secondary mirrors is currently included in the pointing model, primarily in the term proportional to $\sin z$.

The pointing corrections required for primary and secondary tilts ϵ_p and ϵ_s and relative translation ζ are given by the following formulae, in the notation of Schroeder (1987). A rotation of the secondary by ϵ_s causes a displacement of the image in the focal plane of $2\epsilon_s(d + f_1\beta)$, where d is the separation of the primary and secondary mirrors, f_1 is the focal length of the primary and $f_1\beta$ is the back-focal distance. This corresponds to a pointing error of $\Delta_s = 2\epsilon_s(d + f_1\beta)/f = 2k\epsilon_s$, where f is the focal length of the two-mirror system and k is the ratio of the heights of rays at the margins of secondary and primary. For the WHT, $\Delta_s = 0.4607\epsilon_s$ if the two quantities are in the same units. A relative translation of the two mirrors by ζ perpendicular to the optical axis results in an image motion in the focal plane of $-\zeta(d + f_1\beta)/f_2$ (where f_2, the focal length of the secondary mirror, is < 0), so the pointing error is $\Delta_t = -\zeta(d + f_1\beta)/f_2 f = -k\delta/f_2$. $\Delta_t = +15.25\zeta$ for Δ_t in arcsec and ζ in mm. Finally, the effect of

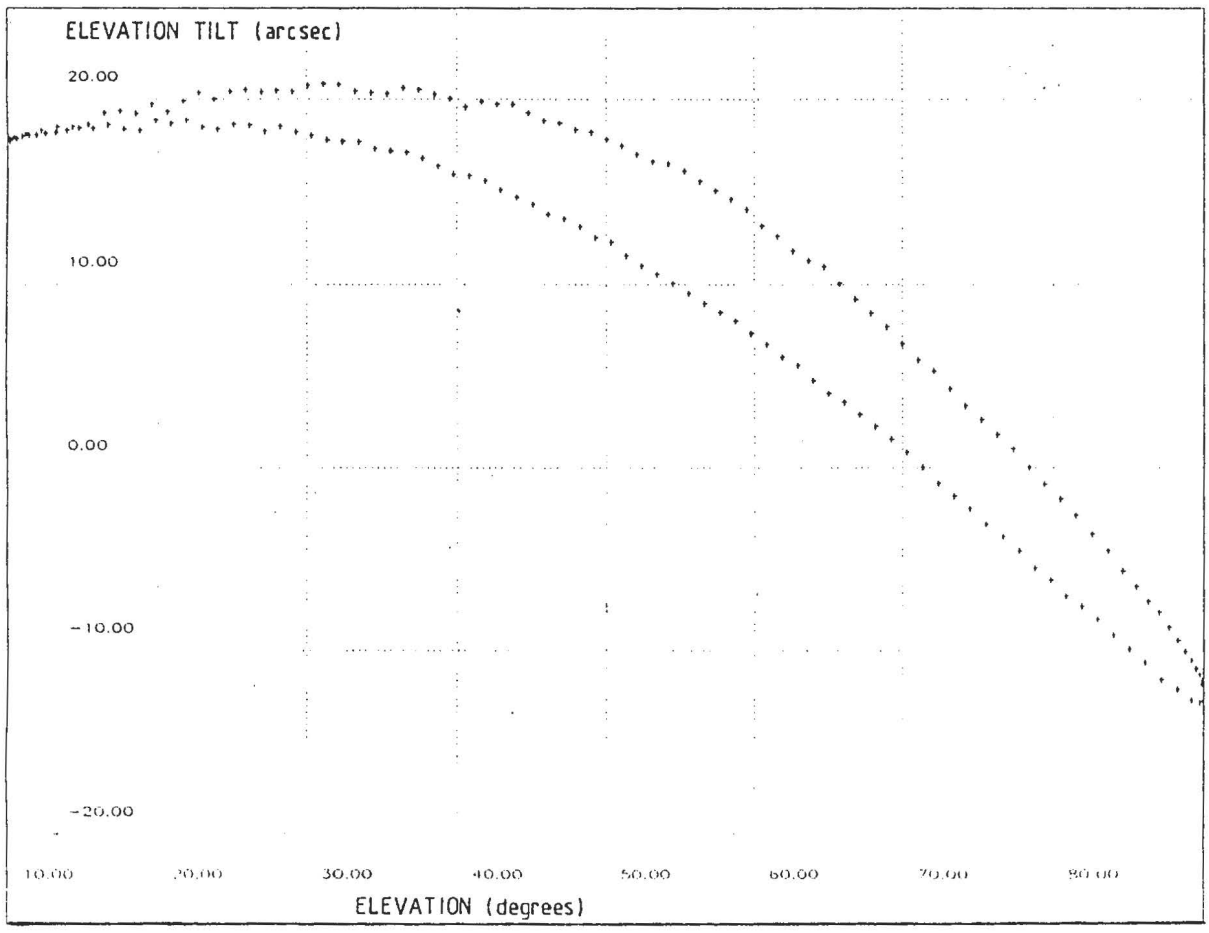

Figure 5: The variation of secondary tilt in elevation with elevation for the William Herschel Telescope. The telescope was driven from the zenith to an elevation of 10° and back. Note the hysteresis effect.

tilting the primary mirror by an angle ϵ_p is an image movement in the focal plane of

$$2\epsilon_p d + 2\epsilon_p(d + f_1\beta) + 2\epsilon_p d(d + f_1\beta)/f_2 = 2\epsilon_p f$$

The corresponding pointing error is $\Delta_p = 2\epsilon_p$, as expected for a single-mirror telescope.

3.9 Derotation Optics

In order to correct field rotation for stationary instruments mounted on the Nasmyth platforms, optical derotators consisting of two Dove prisms and a flat mirror are used (Bingham 1984). These are mounted on the instrument rotators and are driven by the TCS. The derotators are aligned using the altitude axis as a reference, but small residual errors remain to be corrected by the TCS. A first-harmonic term is introduced if the components of the derotation optics are not in accurate relative alignment; a second-harmonic term corresponds to a tilt of the whole assembly with respect to the axis of rotation. For an input beam along this axis, the path of an image in the focal plane of the telescope may be described as follows:

$$x_A = x_0 + a\cos(\rho - \rho_1) + b\cos(2\rho - \rho_2)$$

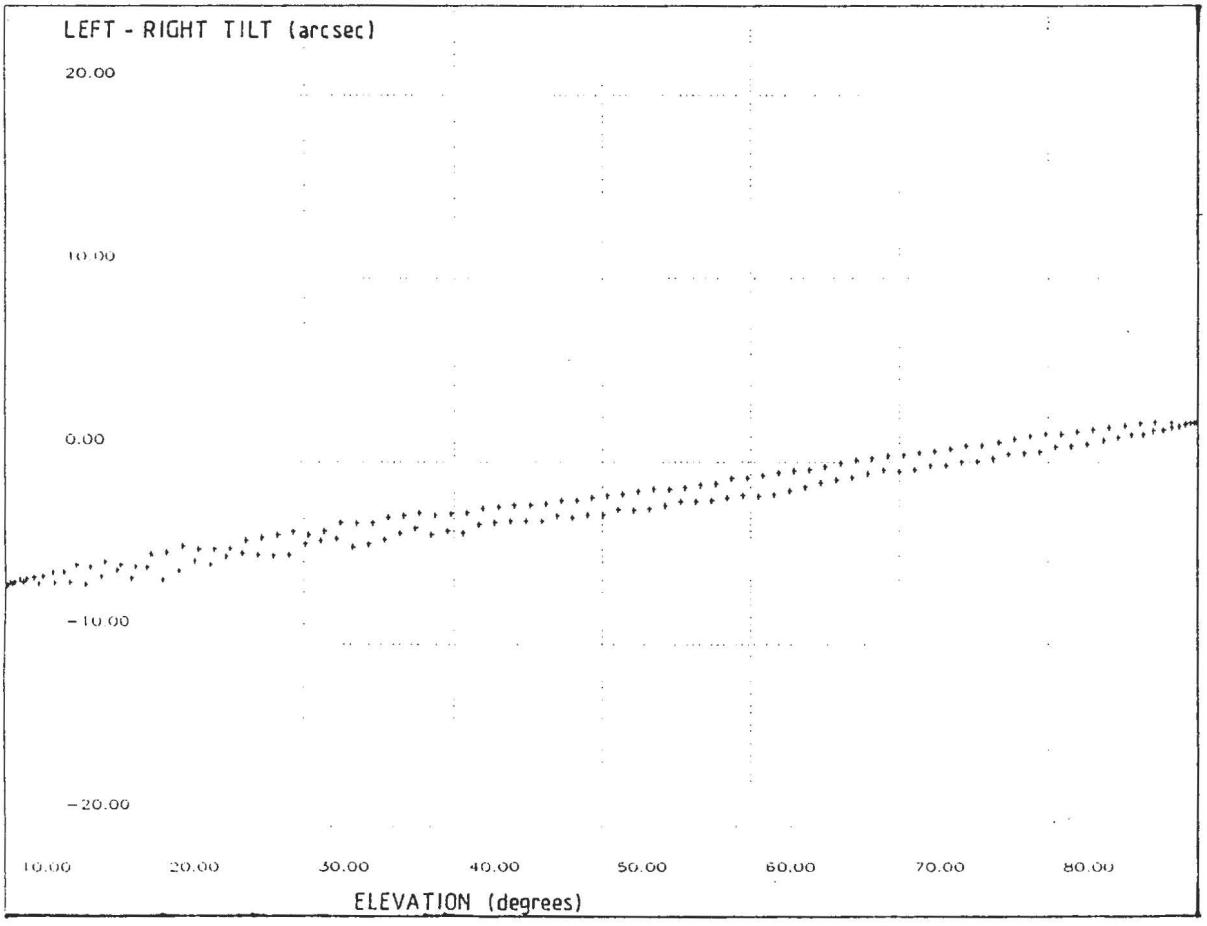

Figure 6: The variation of left-right secondary tilt with elevation for the William Herschel Telescope. The telescope was driven from the zenith to an elevation of 10° and back. Hysteresis also occurs in this direction, although much less than in elevation.

$$y_A = y_0 + a\sin(\rho - \rho_1) + b\sin(2\rho - \rho_2)$$

where ρ is the mount position angle of the instrument rotator and a, b, ρ_1 and ρ_2 are constants. This is the sum of two circular motions, with periods of 180° and 360° in mount position angle. In practice, however, the measured second-harmonic term is a mixture of two effects: the tilt of the optical assembly with respect to the rotation axis and the misalignment of the input beam with that axis. Their superposition is still a circle, and it is always possible to find a position in the field where the image is stationary (the "rotator centre") provided that the first-harmonic term is zero.

These errors are measured by imaging a star onto an autoguider or acquisition camera whose field includes the centre of rotation and logging its position periodically as the derotation optics are turned through a full revolution. An example of a measured track is shown in Figure 7. A correction is implemented as an offset in the focal-plane coordinate system: residuals are plotted in Figure 8.

3.10 Focus

The focus of the telescope depends on temperature (through expansion of the structure), on elevation and on the optical thickness of filters and other components in the beam above the focal plane. The focus value input by the user is a virtual position, whose value does not change with these quantities and which should depend only on the focal station. It is compensated for expansion using temperatures measured by a pair of platinum resistance thermometers on the upper Serrurier trusses which are connected to a Camac ADC module. A linear model is then used to correct the demand focus position. No significant variation of focus with elevation has yet been detected, although provision has been made for an appropriate model. Finally, the focus correction for above-slit filters, polarization elements and similar components are input using the `DFOCUS` command. This may be issued automatically from the system computer when the component is inserted into the beam.

3.11 Autoguiding

In order to correct for irreproducible tracking errors, two types of detector may be used to provide autoguiding signals: off-axis autoguiders and acquisition cameras (which view the spectrograph slit jaws). The methods used to autoguide the WHT are described in detail in *AG* and only a brief summary is given here.

Both types of detector measure image centroid positions, which are sent to the TCS at intervals between 0.1 and 10 s. These are converted from pixel coordinates to the TCS focal-plane system, correcting for the orientation of the guide probe if necessary, and finally rotated to mount AE and added to the position demand. The accumulated autoguiding corrections are stored separately as tangent-plane coordinates in the mount system, rather than being used to update the target right ascension and declination. This reflects the fact that, in normal use, the autoguider is maintaining the image of a given position at a fixed point on the instrument.

3.12 Pointing Calculations

This section outlines the sequence of calculations which perform the pointing corrections described earlier. The treatment by Wallace (1990) is followed closely. The pointing calculations can be divided into those done once (on startup, irregularly when the parameters affecting them are altered or on change of target) and those performed in three loops running at 1/300, 1 and 20 Hz. Unit vectors and matrices are used throughout for efficient and rigorous computation.

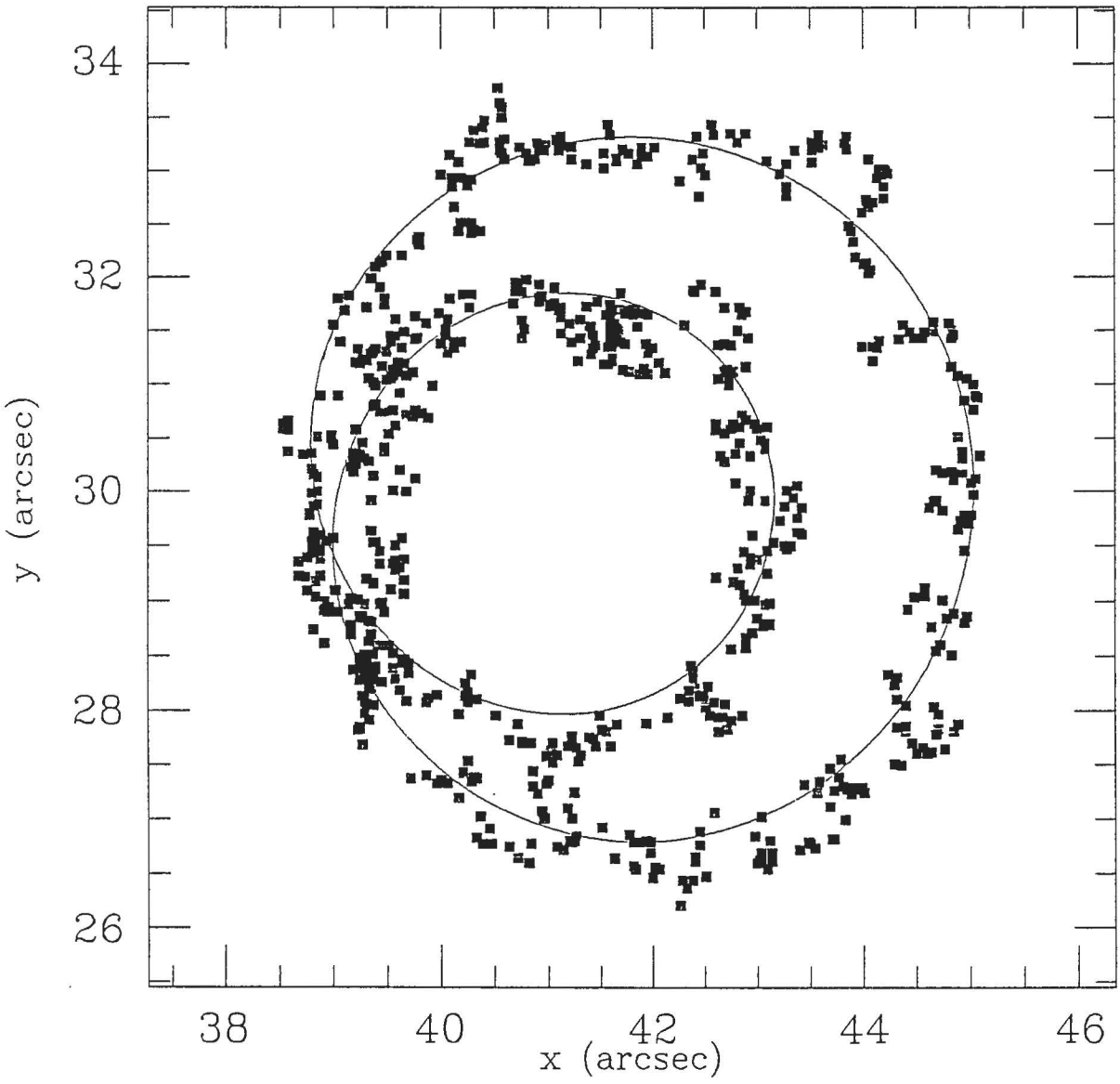

Figure 7: The track of an image on the autoguider at the UES Nasmyth focal station of the WHT during a full revolution of the derotation optics, without the corrections described in the text. The autoguider was placed at the approximate centre of rotation for this test. Note the first and second harmonic components. The best fit to the model in the text is also shown.

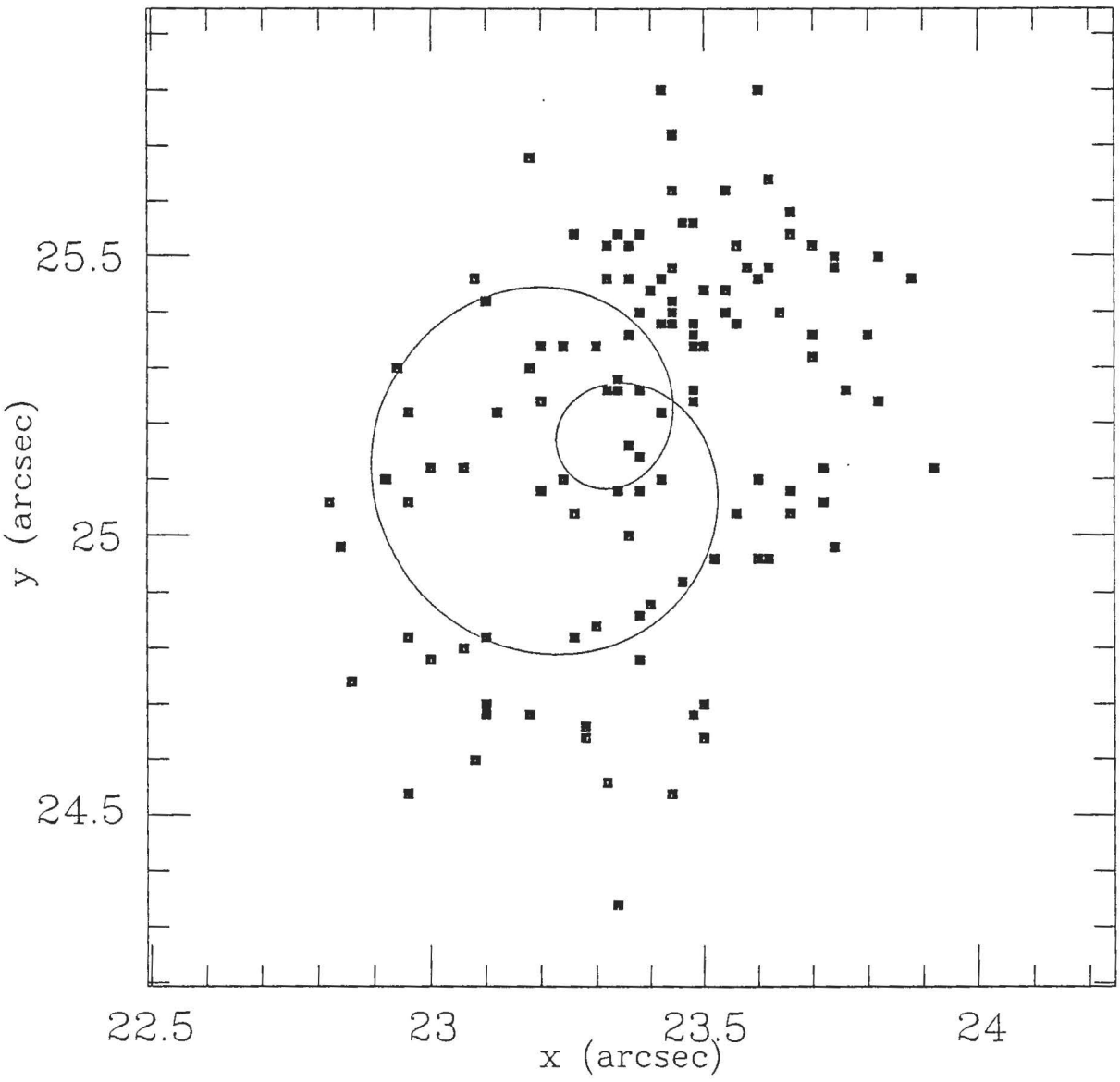

Figure 8: The track of an image on the autoguider at the UES Nasmyth focal station of the WHT during a full revolution of the derotation optics, with the corrections described in the text. The systematic first and second harmonic errors are negligible, but there is some random scatter due to residual tracking drift during the test, and to poor seeing.

3.12.1 Startup

When the TCS starts up, the default values of UT1−UTC and polar motion are calculated from the extrapolation formulae given in IERS Bulletin A. They may be overridden at any time thereafter.

3.12.2 Startup and on change of input parameters

A set of calculations is done at startup and thereafter only when relevant parameters are changed:

- Evaluation of the refraction coefficients $R_A - R_E$, which depend on pressure, temperature, humidity and wavelength.
- Correction of latitude and longitude for polar motion.
- Derivation of the rotation matrix which corrects for azimuth axis tilt.
- Calculation of the constant of diurnal aberration.

3.12.3 Source change

The operations done once, on change of target, are:

- Correction of space motions to the current epoch.
- Formation of the precession matrices needed to convert from FK4 input coordinates to FK4, B1950.0 or FK5 input coordinates to FK5, J2000.0, as appropriate.
- For a blind offset only, conversion of accumulated handset corrections to collimation corrections.

3.12.4 Slow loop: target independent calculations

A number of quantities which change slowly and which are independent of the target being observed are calculated once every 300 s. These are: TDT and TDB, Julian and Besselian epochs and the equation of the equinoxes.

3.12.5 Slow loop: target-dependent calculations

The other portion of the slow loop calculates the parameters needed to convert from mean to apparent place (precession and nutation matrices and aberration vector). These depend on the input coordinate system and the current time, but not on the target position, to which they are applied at higher frequency.

3.12.6 Medium-frequency loop

The function of the medium-frequency (1 Hz) loop is essentially to derive a pair of matrices M_{UA} and M_{AM} which perform the transformation of a unit vector pointing at the target from user coordinates (U) to apparent coordinates (A) and from apparent to mount coordinates (M), respectively. These are then applied at the full loop rate. This avoids the need to re-evaluate pointing corrections which do not change abruptly, but retains the ability to offset the telescope rapidly by changing the target position or collimation corrections. In addition, the medium-frequency loop is used to derive the displayed telescope position in a variety of coordinates systems.

M_{UA} and M_{AM}, called "osculating transformation matrices" by Wallace (1990) are determined as follows:

1. Generate three unit vectors around the target position.

2. Transform them through the relevant portion of the pointing flow.

3. Solve for the matrix that precisely transforms the input to the output vectors.

The matrix would be orthogonal for pure rotations, but some of the pointing corrections (*e.g.* refraction) cannot be modelled in this way. The matrix gives a smoothly changing transformation which should be accurate for any vector close to the target.

The computations included in M_{UA} are:

- FK4 to FK4 B1950.0, using the precession matrix calculated on source change.
- FK4 B1950.0 to FK5 J2000.0, or
- FK5 to FK5 J2000.0.
- FK5 J2000.0 to geocentric apparent.

Therefore,

$$v_A = M_{UA} v_U$$

where v_A and v_U are unit vectors in user and apparent $\alpha\delta$ coordinates.

The terms in M_{AM} are:

- Rotation from (α, δ) to $(-h, \delta)$ (by the local apparent sidereal time).
- Diurnal aberration.
- Rotation to (A, E) (by $\pi/2 - \phi$ about the elevation axis).
- Refraction.
- Correction for azimuth axis tilt.

and,

$$v_M = M_{AM} v_A$$

where v_A is a unit vector in the mount coordinate system.

In addition to transforming the three probe vectors in order to derive M_{UA} and M_{AM}, the medium-frequency loop does the same for the precise target position. The results of intermediate stages in the computation are used to generate the displayed telescope position in various coordinate systems.

3.12.7 Fast loop

The fast (20 Hz) loop performs the following operations:

1. Get UTC and calculate UT1 and local apparent sidereal time.

2. Work out the UTC interval since the start of the track.

3. Apply handset xy, $\alpha\delta$ or $\sigma\tau$ increments accumulated since the last cycle to the running total.

4. Add offsets, handset corrections and non-sidereal tracking corrections to the target position. and generate a unit vector v_U in the user coordinate system.

5. Correct the autoguider reference position for $x_A y_A$ or rotational offsets since the last cycle.

6. For the current and next cycles:
   (a) Apply M_{UA} and M_{AM} to generate a unit vector in the mount coordinate system, v_M.
   (b) Work out the collimation corrections which are specified in the focal-plane (x_A, y_A) system and rotate them to mount (A, E). These are aperture offsets, autoguiding errors and the corrections for misalignment of the derotation optics.
   (c) Add the collimation corrections which are specified in (A, E), that is the azimuth collimation error, non-perpendicularity of azimuth and elevation axes, harmonic terms and blind offset model. The collimation errors are applied by calculating the azimuth and elevation corrections ΔA, ΔE from the tangent-plane offsets σ, τ using the formulae given earlier and rotating the unit vector by these amounts.
   (d) Correct for elevation flexure.
   (e) Calculate demand A and E from the unit vector and apply index errors.
7. The demand positions for the next and current cycles are differenced to derive a velocity prediction.
8. The demand mount position angle is derived by constructing a vector in the user coordinate system which is orthogonal to the target vector and parallel to the projected north-south direction. This is transformed into mount coordinates by multiplying by the matrices M_{UA} and M_{AM} and the angle between it and a vector along the direction of the local vertical in the focal plane is generated.
9. A correction is then made for collimation errors, which are not included in the matrices.
10. The calculation is also done for the current and next cycles, in order to derive a velocity.

Rotator index errors are included in the encoder model.

3.12.8 Sequence of operations on change of source

The use of cascaded loops requires some care on change of source, in order to avoid using matrices derived for one object in calculations for another, especially as only the fast loop is uninterruptible. The order of operations is as follows:

1. One-off calculations are done by the user interface command routine.
2. The slow loop is then triggered immediately. Since it can be interrupted, its results are not made accessible to the rest of the TCS until the calculations are complete (meanwhile, the results of the last cycle are used).
3. The medium-frequency loop is then triggered in a similar way. When it has completed, it instructs the relevant mechanisms to move by modifying their command fields (see below).
4. Finally, the next cycle of the fast loop detects that a source change has happened, and performs a number of special operations:
   (a) Set the new target position.
   (b) Clear positional, aperture and rotator offsets and handset corrections.
   (c) Store the UTC at the start of the track in order to apply non-sidereal tracking corrections.
   (d) Stop autoguiding.
   (e) Recalculate the sky position angle if the rotator is being driven so as to minimise the slew time or to set the spectrograph slit vertical at the start of an observation.
   (f) Decide which way to move the azimuth and rotator if there is more than 360° of travel and the demand position is ambiguous (the closest position is always selected).

4 Drives and Encoders

4.1 Mechanism control

4.1.1 General

Each mechanism is described within the TCS by a record containing the following fields:

Demand position The desired position for the mechanism in the mount coordinate system, either updated continuously during a sidereal track or set to a constant value if a mechanism is to be moved to a given position and stopped.

Actual position The position of the mechanism in the mount coordinate system (corrected for any errors peculiar to the encoding system). This should be equal to the demand position if the telescope is tracking or stopped in position.

Command field The field set by the user-interface command routines in order to instruct the mechanism to move, stop or zeroset.

Status field The field which records whether the mechanism is: moving or stopped, following or not following, in position or not and zeroset or not.

Servo constants A general servo algorithm is used for the main mechanisms. This allows for:

1. A velocity demand proportional to the square root of the position error at large distances from the target.
2. A PID controller for small errors. The velocity demand for a sidereal track is the sum of that predicted by the pointing loop and the output of the PID algorithm.

Limits Software limits on position (positive and negative), velocity and acceleration can be set, although some (*e.g.* the rotation limits for the Nasmyth turntables) are not often used. If the demand position is outside a software limit, then the mechanism is stopped and an alarm is triggered; excessive velocities and accelerations are clipped.

Stopping radius This is the tolerance within which a mechanism will be set by a command to move to position and stop.

In-position radius The in-position radius defines the tolerance within which observing is possible for a moving mechanism. If the position error is less than this value, then the mechanism is said to be "tracking".

"Following" means that the position of the mechanism is being updated continuously. For altitude, azimuth, field and dome rotation this is done during a sidereal track; the focus is adjusted in response to changes in temperature.

The TCS performs mechanism control in three logical stages:

1. The user-interface routines (one for each of the commands listed in Appendix C) either initiate the continous updating of demand positions required if the mechanisms concerned are following or set a constant value if not. They then modify the appropriate command and status fields.

2. The pointing calculation is executed in four loops (once/source change, 1/300, 1 and 20 Hz) as described in Section 3 if a sidereal track is in progress. All this does is to update the demand position.

3. A second set of routines running at 20 Hz reads and decodes the time and encoders, looks at the command and status fields for each mechanism, and at the demand and actual positions, calculates velocity demands, checks for software limits and outputs appropriate commands to the drives.

4.1.2 Rotator modes

A number of different ways of controlling the field rotation have proved to be useful in practice:

1. The sky position angle is specified explicitly, as discussed earlier.
2. On change of target, the demand sky position angle is recalculated to cause the minimum rotation from the present position. Thereafter, sidereal tracking continues as in the first option.
3. The mount position angle is specified. The main applications are: to keep a spectrograph slit vertical so that differential refraction does not cause significant light loss and optical testing, where the test equipment should not rotate with respect to the mirrors. Off-axis autoguiding is not currently possible in this mode, although modifications to allow it over a limited range of rotation are described in *AG*.
4. The sky position angle is reset on change of target to place the slit vertical, but thereafter to track at sidereal rate. This allows autoguiding whilst minimising the effects of refraction.

At the Nasmyth foci, three modes are possible:

1. The instrument is stationary and derotation optics are used to maintain the field orientation. The field then rotates by twice the change in mount position angle.
2. The instrument is stationary and the derotation optics are not fitted (the situation where they are fitted, but stopped, is not identical, since there is a constant rotational offset).
3. The instrument is mounted directly on the rotator, as at the other focal stations, and is rotated to track the sky.
4. The instrument is mounted directly, but is rotated to track the Nasmyth flat ($\rho = \pm E$ to a first approximation). This maintains the orientation of the instrument with respect to the telescope optics and is appropriate for optical testing and some interferometric applications.

The TCS treats a Nasmyth focus with and without derotation optics as two separate focal stations, although the same physical drive and encoders are used for both. Different scaling factors are used for position and rate and the pointing models are independent. A stationary instrument without derotation optics is currently treated as a special case of a rotating instrument with a constant mount position angle but this is unsatisfactory in principle (*e.g.* flexure of the rotator is relevant only if the instrument is attached to it).

4.1.3 Wrap problems

Azimuth and Cassegrain field rotation have more than 360° of travel and parts of their ranges are ambiguous. On change of target, the TCS selects the nearest option by default, regardless of the time remaining before a limit is hit (Section 5.2). It is therefore occasionally necessary to rotate by a full turn in order to avoid tracking into a limit or to reset the mechanism if a limit has been hit during observing. This is done using the `UNWRAP` command (Appendix C), which has four modes of operation, depending on the initial state of the mechanism:

1. If the mechanism is tracking normally, and is in its ambiguous range, then the demand position is changed by 360°.

2. If a software limit is encountered during tracking, then the demand position is reset and the mechanism is commanded to move. Offsets and other accumulated corrections are preserved; otherwise the effect is the same as slewing to the target again.

3. If the mechanism is stopped in an ambiguous part of its travel, then it is rotated by 360° and stopped again.

4. If the mechanism is in the process of being driven to a fixed position, then this position is altered by 360° (if possible) and the move continues.

4.2 Encoders

4.2.1 General

Multiple encoding systems are used on the azimuth, elevation and rotator axes. The purpose of the encoder models used by the TCS is to produce estimates of the position of each axis which are independent of the details of the encoding hardware, so that values from different encoders can be combined or compared. Four types of encoder are used:

Absolute These are optical absolute encoders of relatively coarse resolution used primarily to set initial zero-points and thereafter as a check. They are gear-driven and are used on all axes.

Gear The primary encoders used in normal operation are gear-driven optical incremental systems. They are zeroset against the absolute encoders when the TCS starts up.

Tape The azimuth axis is equipped with an inductive tape encoder with four reading heads (Amos *et al.* 1992). This has higher performance than the gear encoder and is likely to become the primary system for azimuth once its stability and robustness have been verified.

Roller The altitude and azimuth axes are also fitted with friction-driven encoders. These have proved to be unsatisfactory and are not currently used.

The raw values read from the encoders are processed through a model which has the following components (not all of which are used for every encoder):

1. Scale and zero-point.

2. A look-up table, which is derived from smoothed tracking data.

3. Sinusoidal and triangular functions of arbitrary period and phase.

4. A correction derived from displacement measurements (see below).

The zero-points of the incremental encoders may be determined in a number of different ways: by comparison with the absolute encoders; by driving the telescope past a reference position where a proximity detector produces a hardware signal to clear the counter or by driving the telescope to one of its hardware park position, which are defined by independent microswitches.

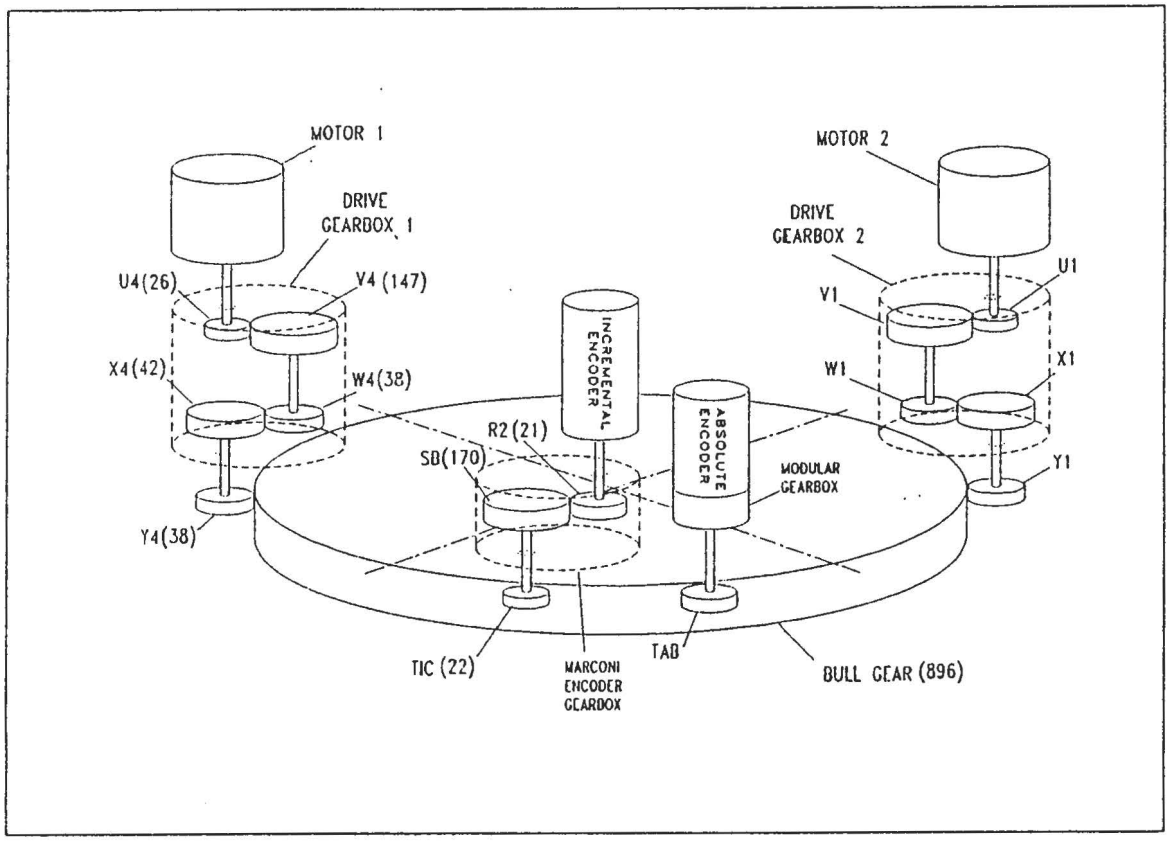

Figure 9: The azimuth drive and encoder gear train (from Amos *et al.* 1992).

4.2.2 Azimuth gear encoder

Fourier analysis of tracking and encoder difference data can be used to identify periodic components and this has been done in detail for the azimuth axis as part of the test programme for the tape encoder (Amos *et al.* 1992). Several obvious spatial frequencies result from the layout of the drive chain and encoder gearing (Figure 9): these are listed in Tables 2 and 3, respectively. The most sensitive way of detecting short-period errors is to difference the gear and tape encoders whilst the telescope is moving very slowly and then to take a Fourier Transform (Figure 10).

The largest systematic error affects the gear-driven encoder on the azimuth axis. The radial hydrostatic support of the telescope is insufficiently stiff to prevent sideways movement. There are two main effects. Firstly, the opposing anti-backlash torques of the two azimuth drive motors cause the telescope to displace sideways by about 50 μm along the perpendicular to the line joining them. Rotation in azimuth then leads to a first-harmonic error. Secondly, there is a sideways movement with the tooth period of the main drive gear (0.4018°). The encoder sees a component of the translation as an apparent azimuth error of amplitude 2 – 3 arcsec (Figure 11). In order to remove these effects, a pair of displacement transducers is used to measure the translation along the appropriate direction. These are mounted on a fixed part of the structure, and impinge on a nominally cylindrical, precision-ground surface on the telescope. Their readings are scaled, averaged (to remove the effects of elliptical distortion of the surface on which they bear) and subtracted from the encoder readings. Figure 12 shows the scaled displacement corresponding to the tracking data in Figure 11. The correction removes approximately 97% of the 0.4018° error, but is still not entirely satisfactory, since additional errors are

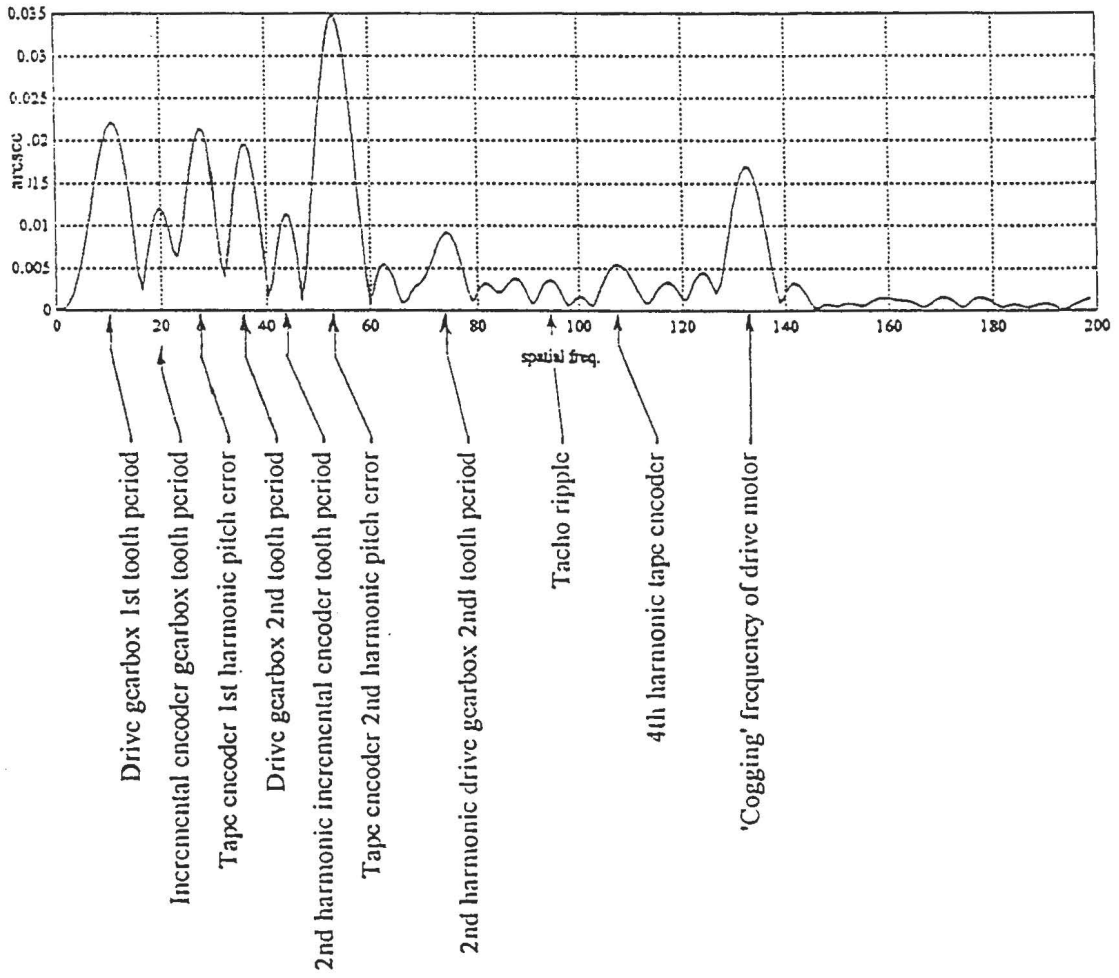

Figure 10: A FFT of the difference between one of the tape encoder heads and the gear encoder in azimuth over a period when the telescope was being driven at a very slow, constant rate. Significant periods associated with both encoding systems are marked. The units of spatial frequency are degrees^{-1}.

Table 2: Characteristic spatial frequencies for the azimuth drive and gear chain.

Component	Calculation	Period (deg)	Detected?
Spur tooth / bull gear	360/896	0.4018	Yes
Spur gear rotation	38 × 0.4018	15.276	No
First stage gear tooth	15.276 / 142	0.1076	No
First stage gear rotation	38 × 0.1076	4.088	No
Second stage gear tooth	4.088 /147	0.0278	Yes
Motor shaft rotation	26 × 0.0278	0.7228	No
First motor cogging frequency	0.7228/(190/2)	7.608×10^{-3}	Yes
First tacho ripple frequency	0.7228/(139/2)	0.0104	?

Table 3: Characteristic spatial frequencies for the azimuth gear encoder chain.

Component	Calculation	Period (deg)	Detected?
Pinion tooth	360/896	0.4018	Yes
Pinion rotation	22 × 0.4018	8.8392	?
Intermediate gear tooth	8.8392/170	0.0520	Yes
Intermediate gear rotation	21 × 0.0520	1.092	Yes

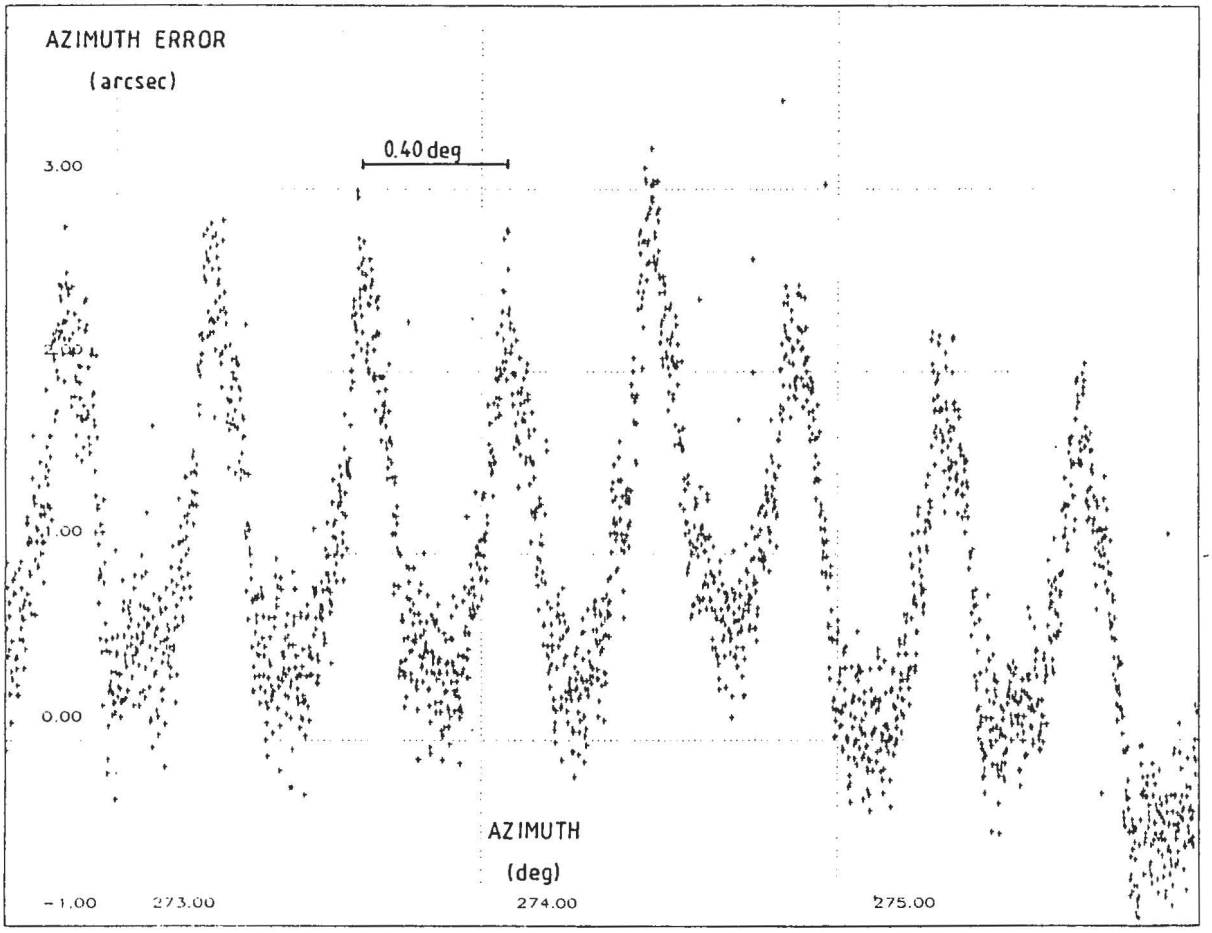

Figure 11: The azimuth component of image motion measured with an on-axis acquisition camera. The gear encoder was used without corrections, in order to show the 0.4° error due to horizontal translation.

introduced because the ground surface is not a perfect cylinder.

Figure 13 shows the residual error in azimuth after subtracting the 0.4° component. The major remaining systematic error is a symmetrical sawtooth with the period (1.09°) of rotation of the second gear in the encoder gearbox and an amplitude of 0.88 arcsec. It is modelled using a triangular function derived from tracking data. An example of a tracking test with all encoder corrections turned on is shown in Figure 14. Note that the error measured on the sky is multiplied by $\cos E$ (≈ 0.62 for this test).

Figure 15, shows an FFT of open-loop tracking errors using the gear encoder. The trace is dominated by three components: the translation error at 0.4018° and the rotation (1.09°) and tooth (0.052°) periods of the second encoder gear. The first two of these are the residuals of the corrections described earlier, and represent roughly 3% and 11% of the original uncorrected error, respectively.

4.2.3 The azimuth tape encoder

The tape encoder deals with the problem of translation by averaging the readings from heads placed 180° apart, which see equal and opposite effects. The residuals for a single tape head show a first-harmonic component of amplitude 3 arcsec due to the wander of the axis of rotation mentioned earlier and the 0.4018° translational error, but neither of these effects is significant in the mean.

The tape is manufactured with a pitch of 2 mm, and errors at the first (0.038°) and second (0.019°)

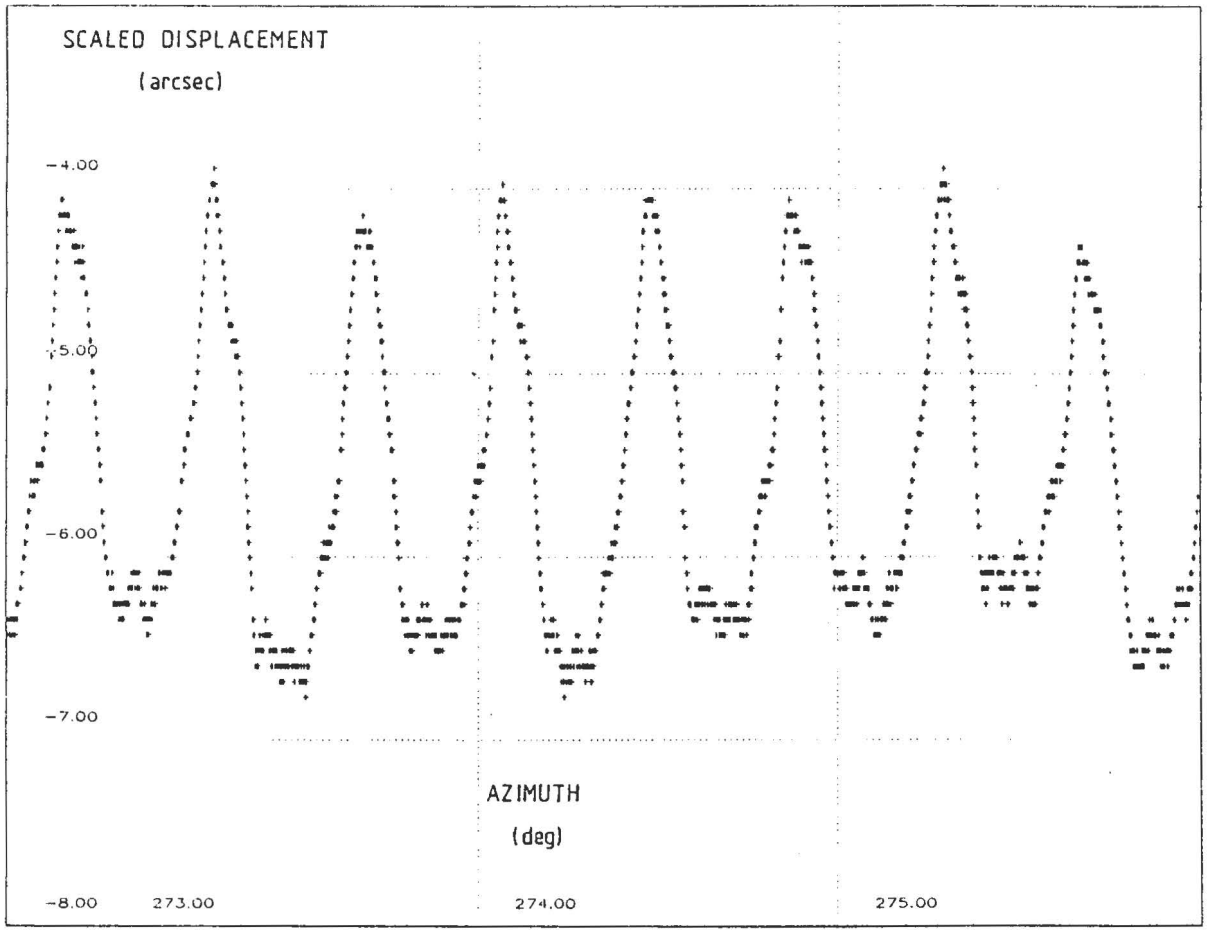

Figure 12: The correction to the azimuth gear encoder reading derived from displacement transducer readings for the data in the previous figure.

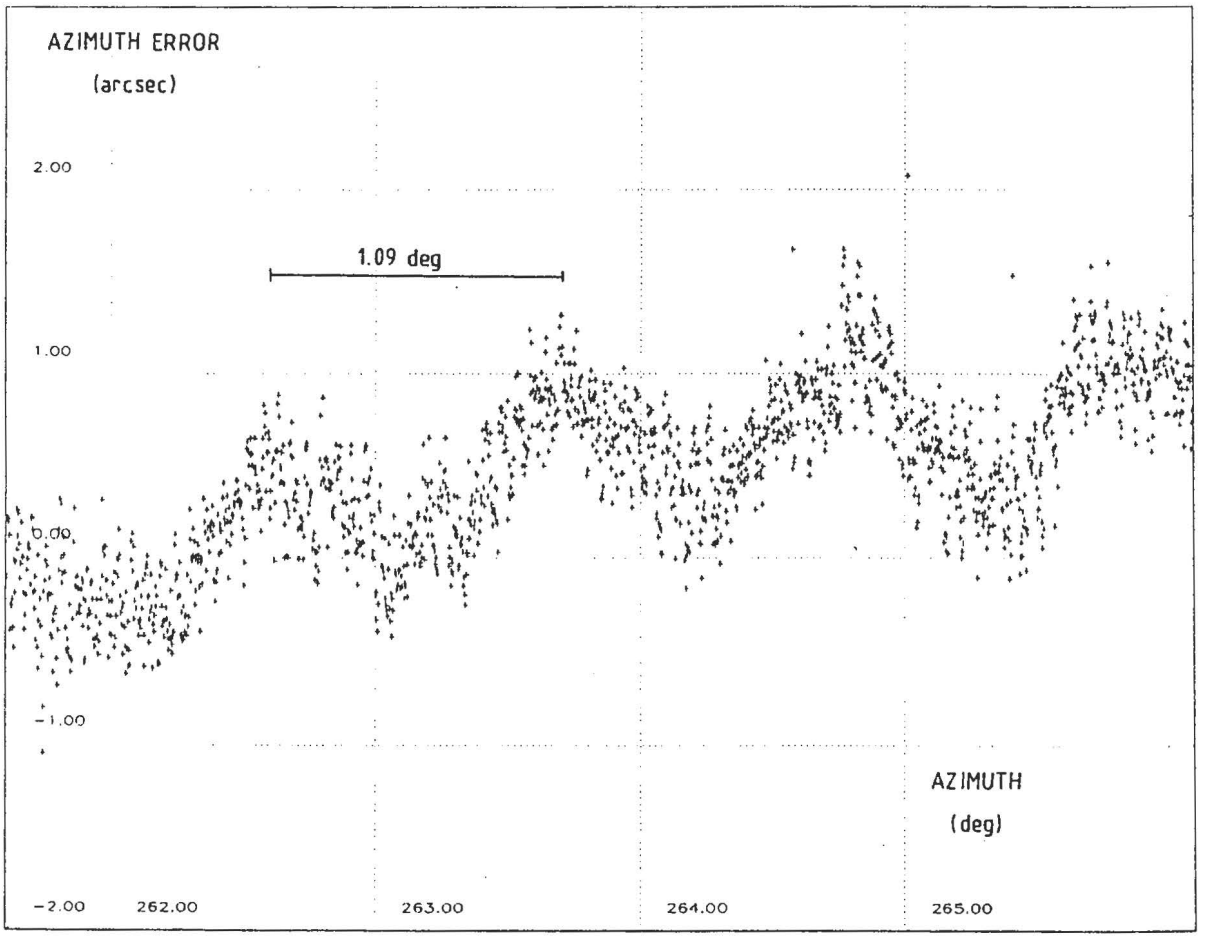

Figure 13: The azimuth component of image motion measured with an on-axis acquisition camera after subtracting the 0.4° translational error from the gear encoder reading. The 1.09° sawtooth corresponding to the rotation period of the second gear in the encoder gearbox is clear in this diagram.

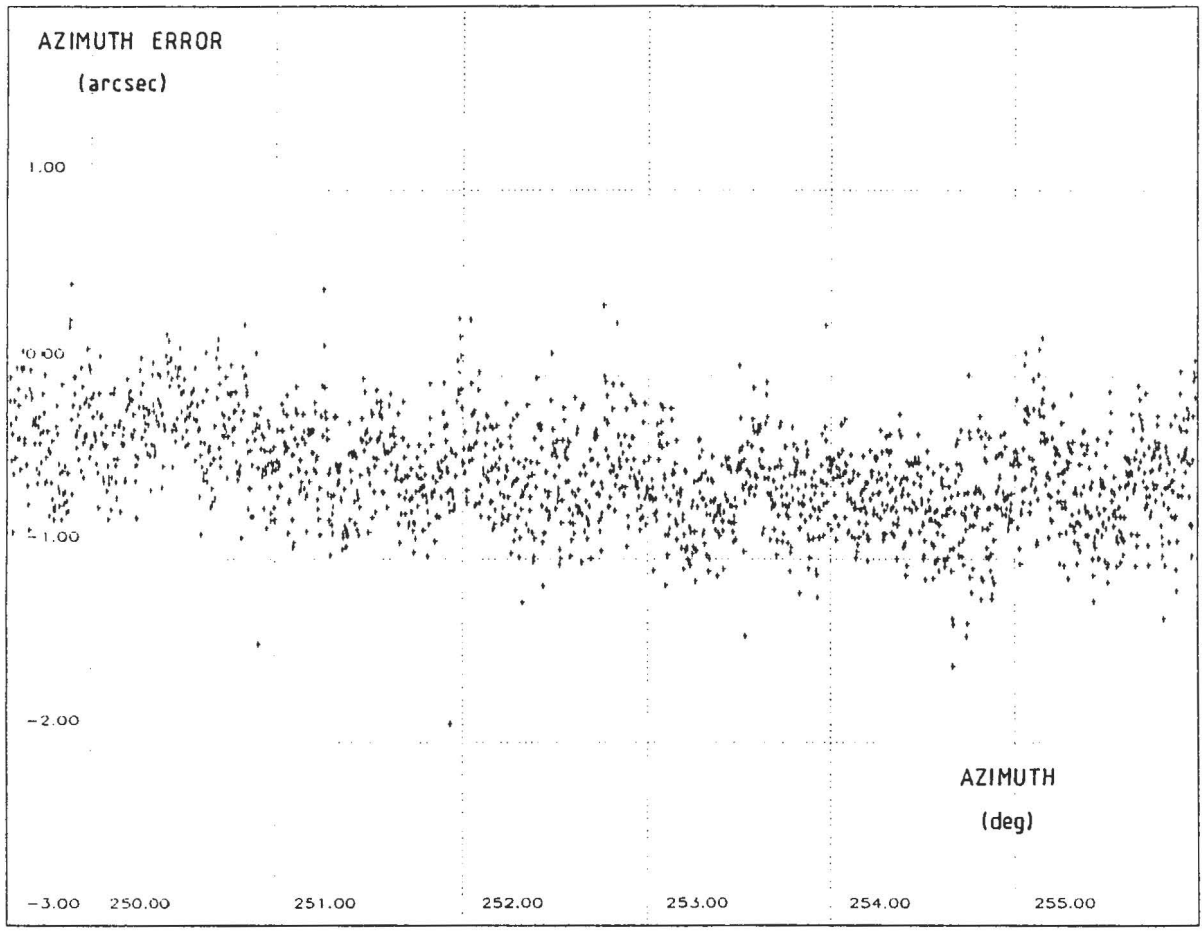

Figure 14: The azimuth component of image motion measured with an on-axis acquisition camera for a track between elevations of 49° and 56°. The gear encoder was used to measure azimuth position, after correction for 0.4° and 1.09° errors. Note that the error measured on the sky is $\cos E \approx 0.62$ of that displayed here.

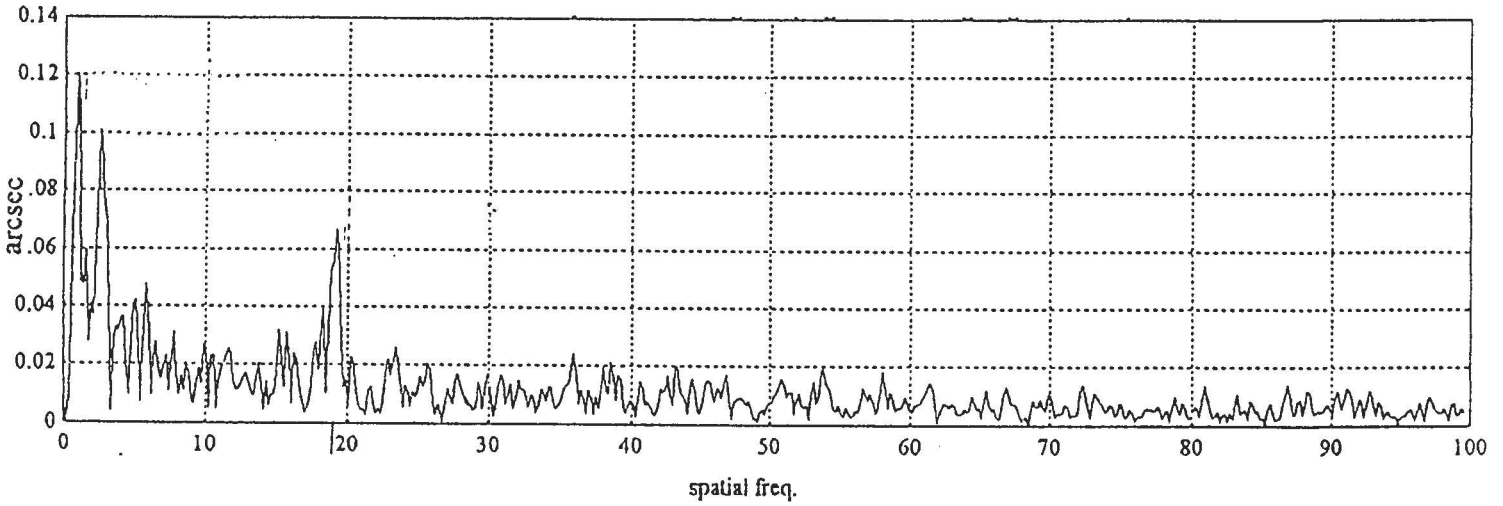

Figure 15: FFT of open-loop tracking errors in azimuth, measured using an on-axis TV camera for the gear encoder. The units of spatial frequency are degrees^{-1}. The three prominent periods are: the residual from the second encoder gear rotation period (0.9 deg^{-1} or 1.09°), the residual translational error at the main drive tooth period (2.5 deg^{-1} or 0.4018°) and the tooth period of the second encoder gear (19.2 deg^{-1} or 0.052°).

harmonics of this period are expected. The r.m.s. pitch errors for a single head are <0.025 arcsec (first harmonic) and 0.036 arcsec (second harmonic) on average, with significant differences between individual heads. When all four heads are averaged, however, these errors are undetectable (<0.01 arcsec and <0.025 arcsec r.m.s., for first and second harmonics, respectively). Large-scale errors are expected from the manufacturing process (these were calibrated before the tape was fitted), from uneven fitting of the tape to the telescope and from the tape join. With no calibration, the maximum discontinuity on the WHT would be averaged to 0.3 arcsec and scale non-linearities are no worse than one part in 20000. The use of empirical look-up tables (implemented in the TCS but not yet calibrated) should lead to further improvements. Models for individual heads should also be introduced in order to allow arbitrary combinations to be used in case of failure.

The superior tracking performance of the azimuth tape encoder is illustrated in Figures 16 and 17 (compare Figures 14 and 15, noting the changes of scale). The tape encoder is free of obvious periodic components (even tape pitch errors) and this test gives a good illustration of current performance limits under optimum conditions. The r.m.s. error is 0.11 arcsec, superimposed on a mean drift of 0.12 arcsec in 36 minutes. During this period, the servo position error was 0.049 arcsec r.m.s. In addition, some contribution to image motion (very roughly 0.05 arcsec r.m.s.) comes from the atmosphere, so a best estimate of the contribution from systematic encoding errors is 0.09 arcsec r.m.s. The tape encoder is also superior on large scales: the r.m.s. residuals in $A \cos E$ from a pointing model fit are typically 0.8 arcsec and 0.6 arcsec, respectively, for the gear and mean tape encoders.

The tape encoder is clearly superior and will become the primary encoding system in azimuth once its stablity and reliability have been fully tested. As a results of the study described in Amos *et al.* (1992) and summarised here, encoders of this type have been selected for the Gemini telescopes.

4.2.4 Elevation encoding

The elevation axis has not been subjected to as detailed an analysis as the azimuth axis, partly because only one encoder is fitted, but also because its systematic errors are much smaller. Part of the reason for this is that translational errors act against gravity, and are therefore much less likely to move the

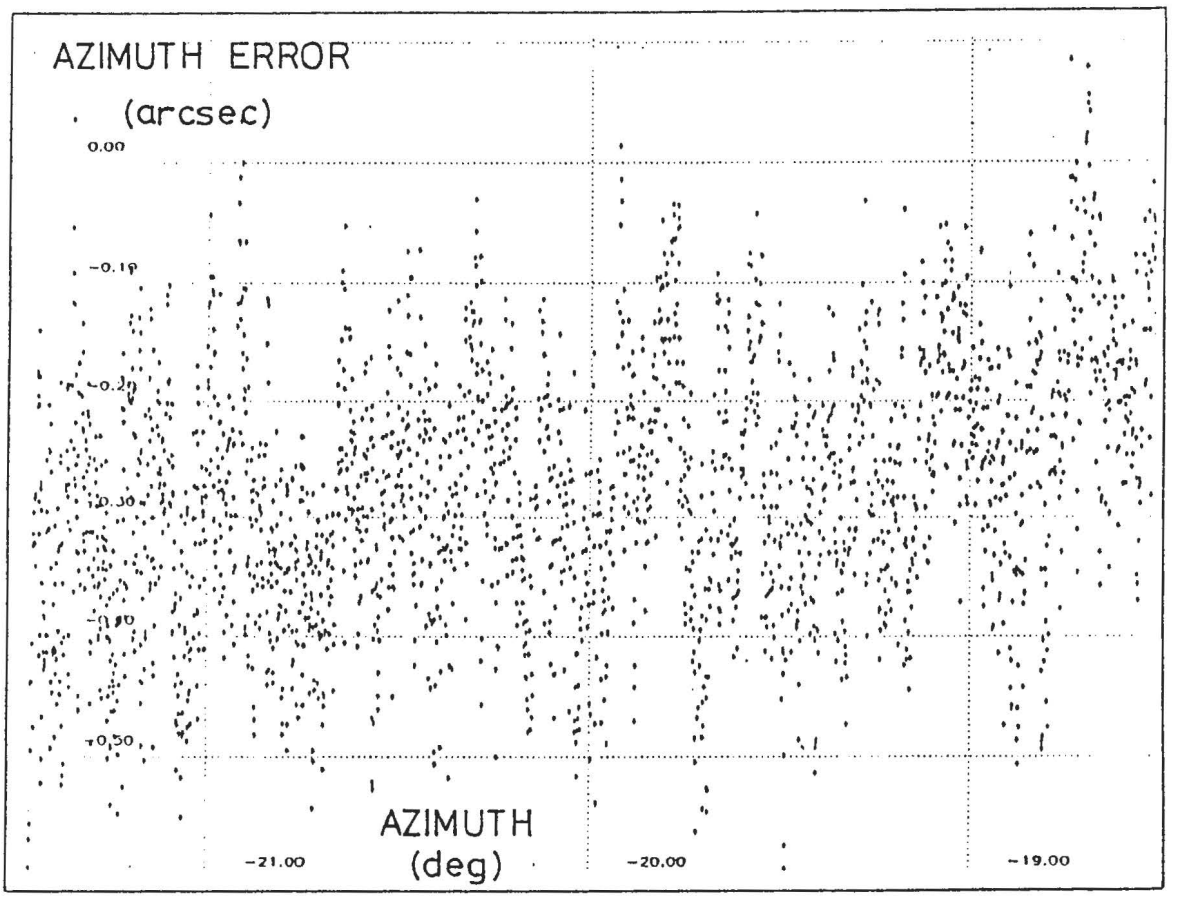

Figure 16: The azimuth component of image motion measured with an on-axis acquisition camera. The mean of the four tape encoder reading heads was used to derive the azimuth position. The duration of the track was 36 minutes and the initial elevation was 45°, so the error measured on the sky is $\cos E \approx 0.7$ of that displayed here.

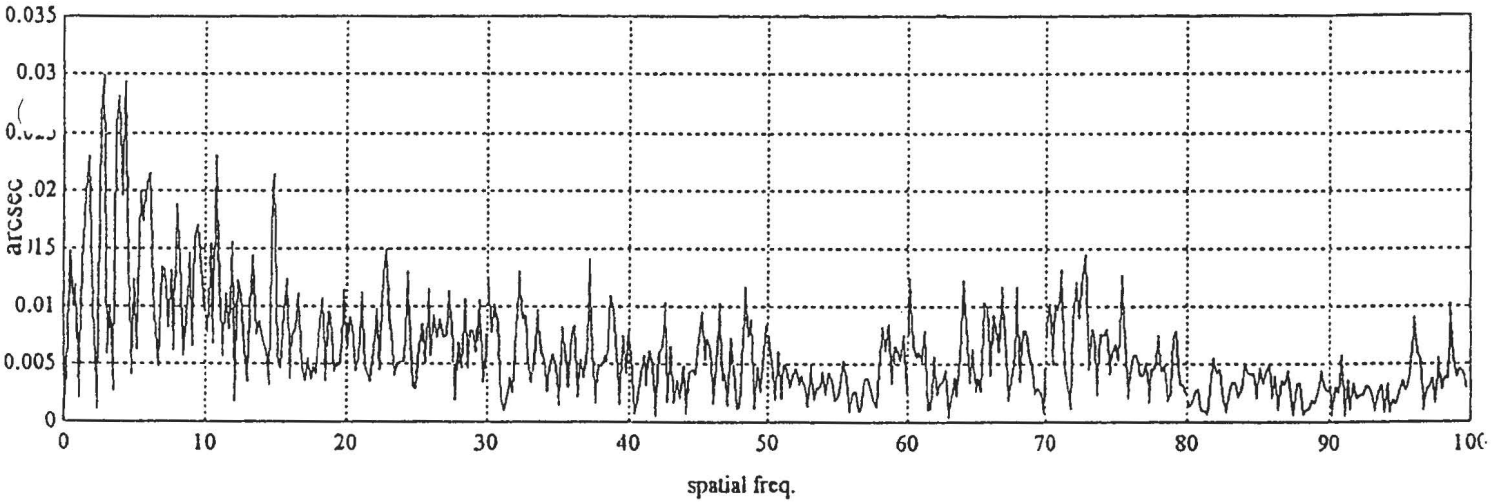

Figure 17: FFT of open-loop tracking errors in azimuth, measured using an on-axis TV camera for the mean of the four tape encoder heads. The units of spatial frequency are degrees^{-1}. Note the change of scale from the equivalent plot for the gear encoder.

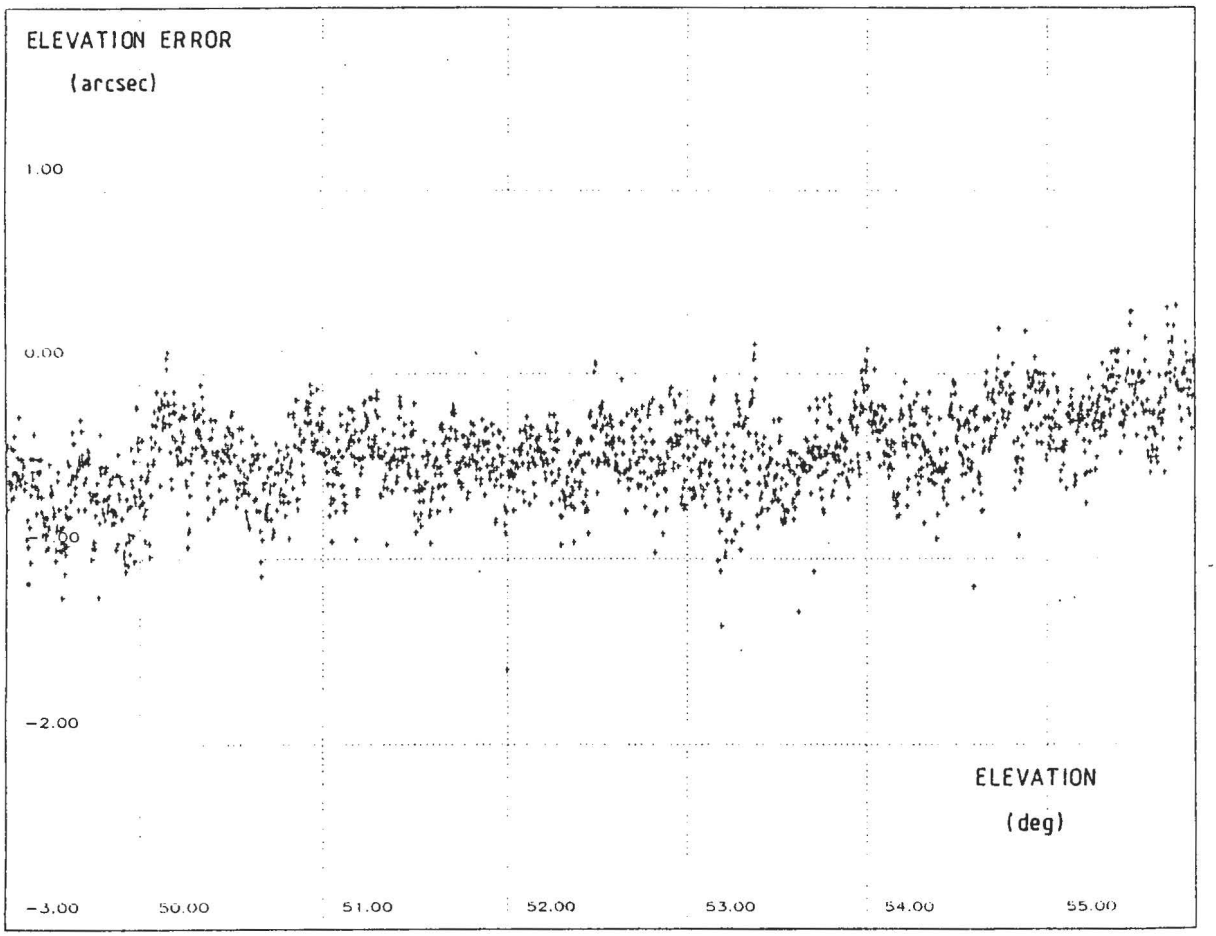

Figure 18: The elevation component of image motion for a tracking test between elevations of 49° and 56°.

telescope. The encoder gearbox is also significantly better than the azimuth equivalent. Figure 18 shows the elevation component of the tracking test in Figure 14.

5 Display Calculations

5.1 The Information Display

5.1.1 General

The Information Display is a set of text pages updated at 1 Hz which describes the current state of the telescope. Its layout is described in detail in Appendix E and the present section is concerned only with non-trivial calculations, particularly those involving limits (section 5.2). The other areas worth noting are the calculation of telescope α and δ and air mass.

The telescope right ascension and declination are only displayed when the position errors are small. The reason for this is that they are derived (in the medium frequency pointing loop) from the *demand* positions, after making a small correction for the servo error, in order to avoid a full reverse transformation. Since the errors are in (slightly) different coordinate systems, this approximation breaks down far from the tracking condition. For similar reasons, there are restrictions on the coordinate system in which the telescope position may be displayed, as described in Appendix C.18. The pointing transformations are carried out in the order: mean FK4, mean FK5, geocentric apparent, topocentric h, δ, as described earlier. The position may be displayed in any system downstream of the input system, but

not in one requiring a reverse conversion.

The formula used for air mass relative to zenith is equation 7.5.34 of Murray (1983) rather than the commonly-used sec z.

5.2 Limit Calculations

The efficient planning of a sequence of observations depends on the ability to calculate the period of time a target can be observed, starting from a given telescope position. This is complicated in the case of an altazimuth mount by the fact that the azimuth and rotator drives have finite ranges of travel. The following calculations have not been published elsewhere, and are therefore given in detail.

5.2.1 Elevation Limits

It is clear that an object is always above the horizon limit if $\delta > \pi - \phi - z$ and always below it if $\delta < \phi - z$. These declinations are $+71.24°$ and $-51.24°$, respectively for the WHT. An object with declinations between these values rises above the elevation limit at an hour angle $-h$, where:

$$\cos z = \cos\delta \cos h \cos\phi + \sin\delta \sin\phi$$

or

$$h = \arccos\left(\frac{\cos z - \sin\delta \sin\phi}{\cos\delta \cos\phi}\right)$$

and sets at hour angle $+h$.

5.2.2 Azimuth

Azimuth is given in terms of hour angle and declination by the expressions in Section 2. Therefore:

$$a = \tan A = \frac{-\sin h \cos\delta}{\sin\delta \cos\phi - \cos\delta \cos h \sin\phi}$$

Squaring this equation gives a quadratic in $c = \cos h$:

$$Bc^2 + Cc + D = 0$$

where

$$\begin{aligned} B &= \cos^2\delta(1 + a^2 \sin^2\phi) \\ C &= -2a^2 \sin\delta \cos\delta \sin\phi \cos\phi \\ D &= a^2 \cos^2\phi \sin^2\delta - \cos^2\delta \end{aligned}$$

The discriminant of this equation is:

$$C^2 - 4BD = 4\cos^2\delta[a^2(\cos^2\delta - \cos^2\phi) + \cos^2\delta]$$

An object *never* encounters an azimuth limit if

$$\cos\delta < |\sin A \cos\phi|$$

or

$$\delta > \arccos(|\sin A \cos\phi|)$$

for a telescope in the Northern hemisphere. The WHT's positive azimuth limit is set at A = 355°, which corresponds to a declination of $\delta = 85.62°$. For declinations less than this value, the quadratic has the solutions:

$$h = \pm \arccos \left\{ \frac{a^2 \sin\delta \sin\phi \cos\phi \pm [a^2(\cos^2\delta - \cos^2\phi) + \cos^2\delta]^{1/2})}{\cos\delta(1 + a^2 \sin^2\phi)} \right\}$$

The first $\pm$ in the solution results from the fact that we have used an equation for $\cos h$ and cannot distinguish between positive and negative hour angles. The ambiguity can be sorted out by inspection or more formally by noting that, since $\sin A = -\cos\delta \sin h / \sin z$ with $-\pi/2 \leq \delta \leq \pi/2$ and $0 \leq z \leq \pi/2$, $\sin A$ and $\sin h$ must have opposite signs. The second $\pm$ occurs because an object may pass through the same azimuth twice. The telescope will, however, be moving in opposite directions in azimuth in the two cases and a limit forbids motion only in one of these.

In the case of the WHT, the positive and negative limits are at A = 355° and A = −175°, respectively. The azimuth velocity is given by:

$$A' = \sin\phi - \frac{\cos\phi \cos z \cos A}{\sin z}$$

The azimuth of an object at A = −175° therefore always *increases* with time and the negative limit is irrelevant for normal tracking. The positive limit can only be encountered when tracking a Northern object below the Pole and this corresponds to the solution:

$$h = + \arccos \left\{ \frac{a^2 \sin\delta \sin\phi \cos\phi - [a^2(\cos^2\delta - \cos^2\phi) + \cos^2\delta]^{1/2}}{\cos\delta(1 + a^2 \sin^2\phi)} \right\}$$

Objects below a certain declination will encounter the horizon limit first. We equate the expressions for $\cos h$ derived for the elevation and azimuth limits. The resulting equation reduces to a quadratic in $s = \sin\delta$:

$$Es^2 + Fs + G = 0$$

where

$$\begin{aligned} E &= 1 + a^2 \\ F &= -2 \cos z \sin\phi (1 + a^2) \\ G &= \cos^2 z (1 + a^2 \sin^2\phi) - \cos^2\phi \end{aligned}$$

For the WHT, A = 355°, z = 80° and $\phi = 28.76°$. This gives the solution $\delta = 70.66°$. Hence the azimuth limit is only relevant for declinations between 70.66° and 85.62° when tracking below the Pole.

5.2.3 The zenith blind spot

The condition for the tracking speed in azimuth to exceed V is $\mu |dA/dh| > V$, where μ is the tracking rate in hour angle (15 arcsec s^{-1}). We define $v = \pm V/\mu$ (= ±240 for the WHT, the sign being negative to the North of the zenith and positive to the South) and solve the equation $dA/dh = v$ for $\cos h$ to give the hour angle at which an object enters the blind spot.

$$\begin{aligned} v &= dA/dh \\ &= \cos\psi \cos\delta / \sin z \\ &= \frac{\cos\delta(\cos\delta \sin\phi - \sin\delta \cos\phi \cos h}{1 - (\cos\delta \cos h \cos\phi + \sin\delta \sin\phi)^2} \end{aligned}$$

This can be rewritten in the form:

$$Hc^2 + Ic + J = 0$$

where (as before) $c = \cos h$ and

$$\begin{aligned} H &= +v\cos^2\delta\cos^2\phi \\ I &= \cos\delta\sin\delta\cos\phi\,(2v\sin\phi - 1) \\ J &= \cos^2\delta\sin\phi - v + v\sin^2\delta\sin^2\phi \end{aligned}$$

The relevant solutions are:

$$\cos h = \frac{\sin\delta(1 - 2|v|\sin\phi) \pm (\sin^2\delta - 4|v|\sin\phi + 4v^2)^{1/2}}{\pm 2|v|\cos\delta\cos\phi}$$

where the + and − signs refer to objects passing South and North of the zenith, respectively.

Solution of this equation confirms that a simple approximation is sufficient to give the range of declinations which is affected by the zenith blind spot. Close to transit:

$$dA/dh \approx \cos\phi/\sin(\delta - \phi)$$

so the condition $|dA/dh| > |v|$ gives $|\delta - \phi| < \cos\phi/v$. For the WHT, this corresponds to $\delta = \phi \pm 0.21°$ or $28.55° < \delta < 28.97°$. In the worst case, the azimuth velocity first exceeds 1 deg s^{-1} at an hour angle of −31 s, so for all practical purposes it can be thought of as entering the blind spot exactly at transit. The telescope will then rotate as rapidly as possible in order to acquire the object at the other side of the blind spot. This takes roughly 3 minutes at full speed.

5.2.4 Rotation limits

We start from the expressions relating sky and mount position angles and parallactic angle given in Section 2. The variation of parallactic angle with hour angle for various declinations is shown in Figure 19. The parallactic angle is undefined at the zenith ($\delta = \phi$, $h = 0$) and the nadir ($\delta = -\phi$, $h = \pi$). In the special cases $\psi = 0$ and $\psi = \pi$, the hour angle is given by:

$\psi = 0 \Rightarrow h = 0$ for $\delta < \phi$ and $h = \pi$ for $\delta > -\phi$.

$\psi = \pi \Rightarrow h = 0$ for $\delta > \phi$ and $h = \pi$ for $\delta < -\phi$.

Curves of $\psi(h)$ (Figure 19) pass through the following points:

$h = \pi$, $\psi = \pi$ and $h = 0$, $\psi = 0$ for $\delta < -\phi$.

$h = \pi$, $\psi = 0$ and $h = 0$, $\psi = 0$ for $-\phi < \delta < \phi$.

$h = 0$, $\psi = 0$ and $h = \pi$, $\psi = 0$ for $\delta > \phi$.

During a sidereal track, a given parallactic angle may occur once, twice or not at all. The condition for 0 or 2 solutions is that the function $\psi(h)$ has extrema. Its derivative at a maximum or minimum is:

$$\psi'(h) = -\cos\phi\cos A/\sin z = 0$$

giving the solutions $\cos A = 0$ or $A = \pm\pi/2$. The expression for $\cos A$ given in Section 2 can be used to reduce this to:

$$\cos h = \tan\delta/\tan\phi$$

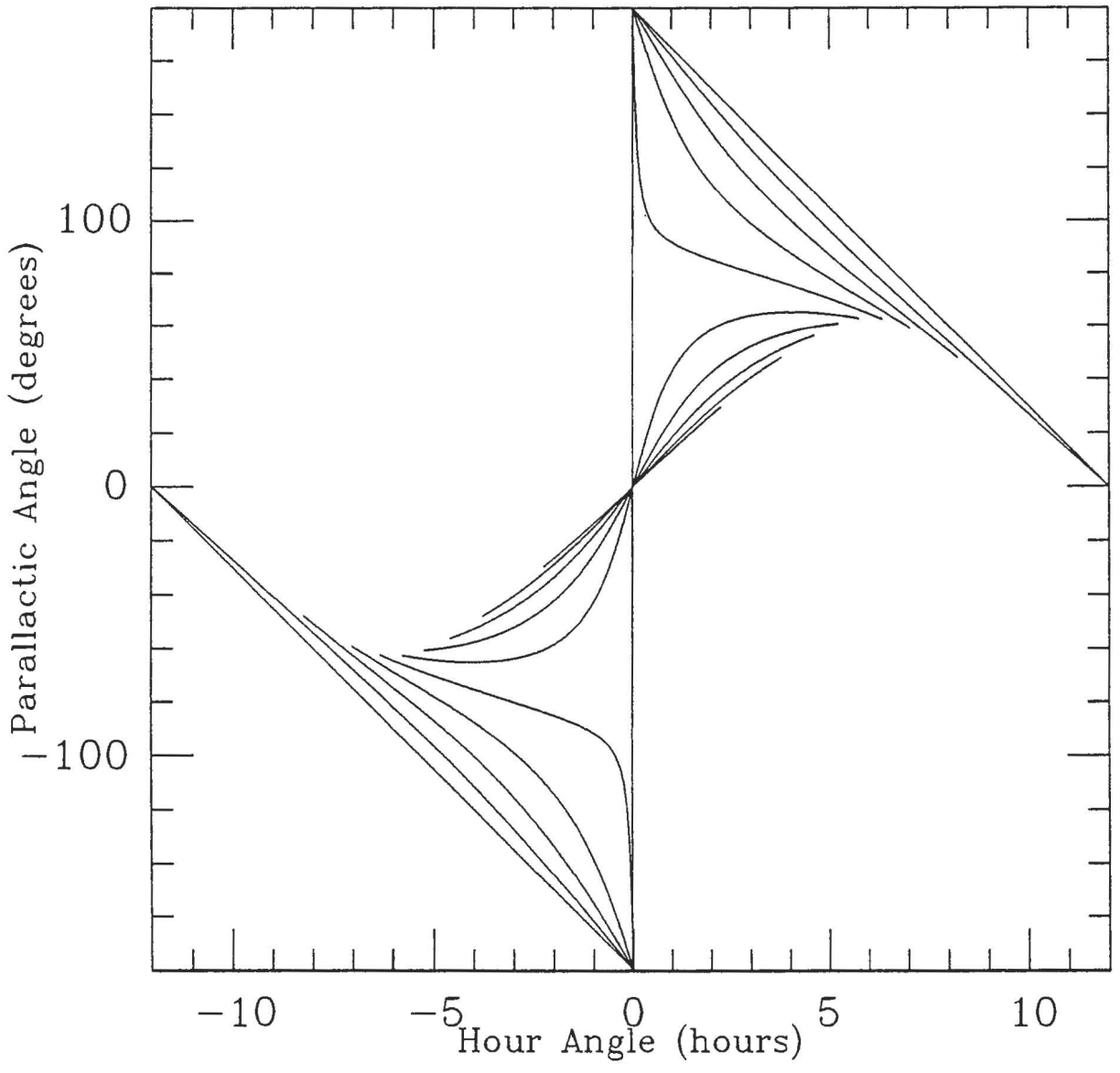

Figure 19: The variation of parallactic angle with hour angle for the latitude of the La Palma Observatory. Curves are plotted for declinations of −45°, −30°, −15°, 0°, 15°, 30°, 45°, 60°, 75° and 90°. The curves are only plotted for observable elevations (> 10°). Declination increases upwards in the top-right quadrant and downwards in the bottom-left quadrant.

which only has solutions if $-\phi \leq \delta \leq \phi$. The maximum occurs for $h > 0$ (A $= \pi/2$), so

$$\sin\psi = -\cos\phi \sin A/\cos\delta = \cos\phi/\cos\delta$$

and the minimum at $h < 0$ (A $= \pi/2$), so

$$\sin\psi = -\cos\phi/\cos\delta$$

Hence:

- There are *no* solutions if $-\phi \leq \delta \leq \phi$ and $\mid \psi \mid < \pi/2$, $\sin\psi > \cos\phi/\cos\delta$ or $\sin\psi < -\cos\phi/\cos\delta$.
- There are *two* solutions if $-\phi \leq \delta \leq \phi$ and $-\cos\phi/\cos\delta < \sin\psi < \cos\phi/\cos\delta$.
- There is *one* solution if $\delta > \phi$ or $\delta < -\phi$.

In order to determine the hour angle corresponding to a given parallactic angle and declination, we start from the relations for $\sin\psi$ and $\cos\psi$ given earlier. These give:

$$p = \tan\psi = \frac{\cos\phi \sin h}{(\cos\delta \sin\phi - \sin\delta \cos\phi \cos h)}$$

This relation can again be squared and rearranged to give a quadratic in c $= \cos h$:

$$Kc^2 + Lc + M = 0$$

with

$$K = (1 + p^2 \sin^2\delta)\cos^2\phi$$

$$L = -2p^2 \sin\delta \cos\delta \sin\phi \cos\phi$$

$$M = p^2 \cos^2\delta \sin^2\phi - \cos^2\phi$$

There are no solutions if $L^2 - 4KM < 0$, which reduces to:

$$\sin^2\psi > \frac{\cos^2\phi}{\cos^2\delta}$$

as before. Otherwise, the possible solutions are:

$$h = \pm \arccos\left\{\frac{p^2 \sin\delta \cos\delta \sin\phi \pm [p^2(\cos^2\phi - \cos^2\delta) + \cos^2\phi]^{1/2}}{\cos\phi(1 + p^2 \sin^2\delta)}\right\}$$

As with azimuth, the use of an equation for $\cos h$ with terms in $\tan^2\psi$ introduces ambiguities (ψ and $\pm\psi + n\pi$ give the same value of p for any integer n). The sign of the arccos function is determined by noting that $h < 0$ if $\psi < 0$ and $h > 0$ if $\psi > 0$. We therefore take + arccos for $\psi > 0$ and − arccos for $\psi < 0$. This leaves the positive and negative roots of the quadratic. For $\delta > \phi$, it is obvious from Figure 19 that there is only one solution for a given parallactic angle. In fact, for $0 \leq \psi \leq \pi$ the roots correspond to parallactic angles ψ and $\pi - \psi$. Similarly for $\delta < -\phi$, $-\pi \leq \psi \leq 0$ and the roots correspond to ψ and $-\psi - \pi$. The situation for $-\phi \leq \delta \leq \phi$ is different: either there are no roots (see above) or both roots correspond to the *same* parallactic angle.

If $\psi = \pm\pi/2$, $p^2 \rightarrow \infty$ and the roots merge. In this case,

$$h = \pm \arccos(\pm \tan\phi/\tan\delta)$$

with the special cases $h = \pm\pi/2$ at the Poles.

Finally, we consider the sense of rotation.

$$\psi'(h) = -\frac{\cos\phi\cos A}{\sin z} = -\frac{\cos\phi\sin\phi\cos\delta}{\sin^2 z}\left[\frac{\tan\delta}{\tan\phi} - \cos h\right]$$

It is clear from this equation that $\psi'(h)$ is always < 0 for $\delta > +\phi$ and > 0 for $\delta < -\phi$. For intermediate declinations, the quadratic has two valid solutions. The condition that its discriminant is zero is $\cos h = \tan\delta/\tan\phi$. Thus the positive root has $\cos h > \tan\delta/\tan\phi$, so $\psi' > 0$. Conversely, the negative branch has $\cos h < \tan\delta/\tan\phi$ and $\psi' < 0$.

The limit conditions are as follows (note that the mount PA and parallactic angle increase in opposite senses):

$\delta > \phi$ $\psi' < 0$ for all hour angles, so the rotator can only track into the positive mount PA limit. Since the rotation is monotonic, the limit will eventually be reached from any starting position provided that the telescope is not stopped by the azimuth or horizon limit, each complete rotation taking 24 hours. It is possible for the telescope to track continuously if $\delta > 85.62°$, in which case the length of the observation is restricted only by the positive mount PA limit (admittedly a somewhat academic example). The positive root of the quadratic applies if $|\psi| > \pi/2$, otherwise the negative root.

$-\phi < \delta < \phi$ There are no solutions if $|\sin\psi| > \cos\phi/\cos\delta$ or $|\psi| > \pi/2$, in which case no limits can be hit; otherwise both roots give valid solutions and either limit can be encountered provided that the initial value of the mount PA is sufficiently close. The condition is:

$$(\theta - \theta_0) - \arcsin(\cos\phi/\cos\delta) < \rho < (\theta - \theta_0) + \arcsin(\cos\phi/\cos\delta)$$

where ρ is the current mount position angle and $(\theta - \theta_0)$ is ranged by adding or subtracting multiples of 2π so that $(\theta - \theta_0) - \rho_\pm$ is in the range $[-\pi, \pi]$. The positive root corresponds to the negative mount position angle limit, and conversely.

$\delta < -\phi$ The positive root is allowed, so $\psi' > 0$ and the rotator can track into the negative mount PA limit. As for $\delta > \phi$, the rotation is monotonic, so the turntable will eventually hit the limit provided that the object does not set first. For a telescope in the Northern hemisphere, such as the WHT, objects with $\delta < \phi$ are not circumpolar, so it is impossible for the turntable to rotate by more than a full turn whilst the object remains above the horizon. The negative root of the quadratic applies if $|\psi| > \pi/2$, otherwise the positive root.

5.2.5 Summary and practical limitations

The effects of the elevation and azimuth limits and of the zenith blind spot are summarised for the WHT in Table 4. Only the elevation limit need be considered in most cases, the possibility of encountering the azimuth limit being restricted to a few northerly objects observed below the Pole.

It should be noted that the azimuth and elevation limits are defined in the *mount* coordinate system and that further transformations are required in order to convert to astronomically-useful (h, δ). Since the index errors for the WHT are included to a good approximation in the encoder model, the difference between mount and topocentric apparent systems is not significant at the level of accuracy required ($\approx$ 1 minute of time). If higher precision is required, then the full pointing model must be included in the calculation. The theoretical radius of the zenith blind spot has been used, and it is likely that tracking will become progressively less accurate as this is approached. For practical purposes, a larger radius might be appropriate. The rotator limits are summarised in Table 5(the same caveats apply as for azimuth and elevation limits).

Table 4: Summary of effective limits for the WHT.

Declination	Effective limit
$\delta < -51.24°$	Never above elevation limit
$-51.24° < \delta < 28.55°$	Rises and sets at elevation limit
$28.55° < \delta < 28.97°$	Rises and sets at elevation limit; passes through blind spot
$28.97° < \delta < 70.66°$	Rises and sets at elevation limit
$70.66° < \delta < 71.24°$	Rises at elevation limit; sets at positive azimuth limit (+ wrap) or elevation limit (− wrap)
$71.24° < \delta < 85.62°$	Always above elevation limit; Sets at positive azimuth limit (+ wrap only)
$85.62° < \delta$	No limits

Table 5: Summary of turntable limits for the WHT ($\psi = \theta - \theta_0 - \rho$, where θ is the sky position angle, θ_0 is an instrument-dependent offset and ρ is the mount position angle of the limit).

Declination	Effective limit
$\delta < -28.76°$	Can hit negative mount PA limit
$-28.76° < \delta < 28.76°$	No limits if $\mid \sin\psi \mid > \cos\delta/0.877$ or $\mid \psi \mid > \pi/2$; otherwise can hit either mount PA limit
$28.76° < \delta$	Can hit positive mount PA limit

6 Diagnostic Procedures

6.1 Pointing tests

In order to measure the terms in the pointing model, a grid of stars with accurately known positions covering all of the accessible parts of the sky is used. The stars are slewed to in sequence and centred on a given point in the focal plane (usually the rotator centre). The values of α and δ in the encoder system are then logged, together with the sidereal time. 100 – 150 measurements are taken, concentrating on the zenith where a number of the terms become easier to distiniguish. The data are analysed using the TPOINT package (Wallace 1989), which uses a least-squares fit to the functional forms give in Table 1 in order to estimate the coefficients. Tests are performed 3 or 4 times a year at each focal station, and after any major mechanical change.

6.2 The CALIBRATE procedure

The CALIBRATE procedure is a short pointing test performed at the start of a night's observing in order to measure the three coefficients which are most likely to change (the azimuth and elevation index errors and the horizontal collimation) and to provide an estimate of the telescope's pointing performance. Seven stars are selected from the standard grid, on the northern or southern meridian (whichever is closer) and with a range of elevations. The telescope is slewed to each star in turn and the operator is invited to centre it on the reference position. The data are logged and automatically analysed as in a standard pointing test, but with all except the three coefficients set to the default values for the current focal station. The values of the coefficients and the r.m.s. fitting error are displayed and the raw data are stored for later analysis. The operator may then accept the new coefficients or revert to the previous or default values. Sky r.m.s. errors significantly in excess of 1 arcsec generally indicate either a breakdown or a slow change in the pointing model.

6.3 Tracking, rotation and encoder performance

The TCS is capable of logging image centroids from an acquisition camera or autoguider and a variety of data concerned with tracking performance at rates up to 20 Hz. These may then be plotted, analysed further (*e.g.* to generate look-up tables or to fit simple functions) or exported using the TCS PLOT utility. Several examples of the use of this technique were given in Section 4.2; it is also used to measure the misalignment of the derotation optics. In order to test the rotator performance at the Cassegrain and Prime foci, an acquisition camera is used to autoguide on a star at the centre of rotation (eliminating tracking errors) whilst an off-axis autoguider simultaneously logs the centroid of an image at the edge of the field.

6.4 Other diagnostic software

Two other utilities are used primarily for hardware testing. GSEXAM sets and reads the global variables used by the TCS for interprocess communication and allows easy access to raw encoder and transducer data. CAMAC_TEST is a test program for the hardware interface which is independent of the TCS.

7 Summary and Future Development

The present paper has summarised the calculations performed by the WHT telescope control system in a manner independent of implementation. The TCS has proved to be accurate and reliable in practical use, and its algorithms are well-tested. Enhancements are planned in two main areas: measurement and control of main mirror position and more sophisticated autoguiding.

Shack-Hartmann testing of the telescope optics has shown that the secondary mirror tilts and translates in such a way as to introduce significant coma away from the zenith (where the alignment is optimised). The coma is a reproducible function of elevation and can, in fact, be predicted from the pointing model and direct measurements of secondary tilt. The tilt of the secondary mirror can be controlled by the TCS, although the drive was not designed for continuous use and may have to be rebuilt. Calculations show that tilt of the secondary alone can remove coma at the field centre without introducing excessive astigmatism at large field radii and this would lead to significant gains in image quality. A second, somewhat easier, possibility is to measure residual tilt on the primary mirror (which is significant at the 0.1 arcsec level and tends to vary slowly with time) and to correct its effects on pointing using the mount.

The aim of improvements to the autoguiding algorithms (see *AG* for more detail) is to allow accurate blind acquisition given an off-axis guide star with an accurately-known displacement from the target. The requirements are:

1. A very accurate calibration of the focal-plane geometry (autoguider probe movement, detector orientation, scale and rotation).

2. An algorithm which predicts the coordinates of the off-axis guide star on the autoguider given its position on the sky and the location of the guide probe. This would be updated continuously in order to allow for time-variable effects such as differential refraction between guide star and target, probe flexure and (for solar-system objects) non-sidereal motion.

The control system for the Gemini telescopes differs from that for the WHT in one major respect: the optical surfaces are under full computer control, some at high speed. The WHT system as described here is entirely adequate to control the mount, field rotation and auxiliary mechanisms of the Gemini telescopes, but requires additional routines to deal with the primary and secondary mirror supports and their associated wavefront sensors. In addition, the hardware and software environment proposed by the Gemini project differs in almost all respects from that used at the WHT. Nevertheless, the work described in this paper goes a considerable way towards solving the problems posed by the new project.

References

Amos, C.S., Churchill, J.E., Fisher, M. & Laing, R.A., 1992. *William Herschel Telescope Inductosyn Tape Encoder Project*, RGO Report RGO-N-008.

Bingham, R.G., 1984. *General Optical Description of the 4.2-m William Herschel Telescope*, La Palma Technical Note **9**.

Hinks, A.R., 1898. *M.N.R.A.S.*, **58**, 428.

Laing, R.A., 1993. *Algorithms for Guide-Star Acquisition and Control of Mount and Optical Surfaces.* RGO Internal Report. (*AG*)

Moyer, T.D., 1981. *Celestial Mechanics*, **23**, 1.

Murray, C.A., 1993. *Vectorial Astrometry*, Adam Hilger, Bristol.

Saastamoinen, J., 1972a. *Bull. Geod.*, **106**, 279.

Saastamoinen, J., 1972b. *Bull. Geod.*, **106**, 383.

Schroeder, D.J., 1987. *Astronomical Optics*, Academic Press, London.

Seidelmann, P.K. (ed.), 1992. *Explanatory Supplement to the Astronomical Almanac*, University Science Books, Mill Valley, California.

Straede, J.O. & Wallace, P.T., 1976. *P.A.S.P.*, **88**, 792.

Wallace, P.T., 1989. *TPOINT – Telescope Pointing Analysis*, Starlink User Note **100**, Starlink Project, Rutherford Appleton Laboratory.

Wallace, P.T., 1990. *Proposals for Keck Telescope Pointing Algorithms*, Starlink Project, Rutherford

Appleton Laboratory.
Wallace, P.T. & Tritton, K.P., 1979. *M.N.R.A.S.*, **189**, 115.

A Notation

ϕ Latitude of the telescope ($\phi = 28°45' 38.1''$)

h Hour angle

α Right ascension

δ Declination

E Elevation

z Zenith distance ($z = \pi/2 - E$)

A Azimuth

ψ parallactic angle

θ Sky position angle

θ_0 Instrument-dependent position angle offset

ρ mount position angle

μ Sidereal tracking rate in hour angle

ξ, η Cartesian coordinates in the tangent plane, parallel to $+\alpha$ and $+\delta$, respectively

σ, τ Cartesian coordinates in the tangent plane, parallel to $+A$ and $+E$, respectively

x, y Cartesian coordinates in the tangent plane along mount position angle 0° and 90°, respectively in the input coordinate system

x_A, y_A Cartesian coordinate system fixed in the focal plane

f_1, f_2, f Focal lengths of the primary and secondary mirrors, and of the Cassegrain combination, respectively

ϵ_p, ϵ_s Tilts of the primary and secondary mirrors with respect to the axis of the instrument rotator(s)

ζ Relative transverse displacement of primary and secondary mirrors

β Back focal distance / f_1

k Ratio of heights of rays at the margins of the secondary and primary mirrors

d Separation of primary and secondary mirrors

Δ_p, Δ_s, Δ_t Pointing errors due to primary tilt, secondary tilt and decentre, respectively

$R_A - R_E$ Refraction coefficients

M_{UA} Matrix to transform a unit vector from user to apparent coordinate system

M_{AM} Matrix to transform a unit vector from apparent to mount coordinate system